2014•2015
FACULTEIT GENEESKUNDE EN LEVENSWETENSCHAPPEN
master in de biomedische wetenschappen

Masterproef

Surface plasmon resonance investigation of gold nanoparticle aggregation on self-assembled monolayers

Promotor :
Prof. dr. Patrick WAGNER

Promotor :
Prof.dr. MICHAEL MERTIG

Copromotor :
Dr. ALFRED KICK

Navid Khangholi
Scriptie ingediend tot het behalen van de graad van master in de biomedische wetenschappen

universiteit hasselt | Maastricht University

De transnationale Universiteit Limburg is een uniek samenwerkingsverband van twee universiteiten in twee landen: de Universiteit Hasselt en Maastricht University.

universiteit hasselt
KNOWLEDGE IN ACTION

Universiteit Hasselt | Campus Hasselt | Martelarenlaan 42 | BE-3500 Hasselt
Universiteit Hasselt | Campus Diepenbeek | Agoralaan Gebouw D | BE-3590 Diepenbeek

2014•2015
FACULTEIT GENEESKUNDE EN LEVENSWETENSCHAPPEN
master in de biomedische wetenschappen

Masterproef

Surface plasmon resonance investigation of gold nanoparticle aggregation on self-assembled monolayers

Promotor :
Prof. dr. Patrick WAGNER

Promotor :
Prof.dr. MICHAEL MERTIG

Copromotor :
Dr. ALFRED KICK

Navid Khangholi

Scriptie ingediend tot het behalen van de graad van master in de biomedische wetenschappen

universiteit hasselt | Maastricht University

Table of Contents

I. List of abbreviations 2
II. Acknowledgments 3
III. Abstract 4
IV. Introduction 5
1. Fundamentals 8
1.1. Introduction to pH value and pH measurement 8
1.1.1. pH electrode sensor 8
1.1.2. Optical pH sensors 9
1.1.3. pH-sensitive polymers as sensor layers 9
1.1.4. Colorimetric pH sensors 10
1.2. Surface Plasmon Resonance 10
1.2.1. Physics of Surface Plasmon 10
1.2.2. Surface plasmon resonance sensor 11
1.2.3. Localised Surface Plasmon Resonance 12
1.2.4. Effect of AuNPs in SPR sensor 13
2. Materials and methods 16
2.1. Gold nanoparticle synthesis 16
2.2. Functionalization of AuNPs with carboxylic groups 16
2.3. SPR measurements 17
2.4. Scanning electron microscopy 19
3. Results and Discussions 20
3.1. AuNP characterization 20
3.2. AuNP-COOH behaviour based pH in bulk solution via UV-VIS spectrsocopy 22
3.3. AuNP-COOH behaviour based pH on different surfaces 23
3.3.1. Ø20 nm AuNP-COOH behaviour based pH within cysteamine hydrochloride and 4-mercaptopyridine 23
3.3.2. SPR for Self-Assembled Monolayers (SAM) and AuNPs (Ø30 nm) 26
3.3.3. P2VP pH-sensitivity with Ø30 nm AuNP-COOH 28
3.3.4. P2VP pH-sensitivity with Ø20 nm AuNP-COOH in microfluidics 30
4. Conclusions and outlook 34
Reference 35

I. List of abbreviations

AuNP	Gold nanoparticle
AuNP-COOH	Gold nanoparticles functionalised with carboxylic group
CA	Cysteamine hydrochloride
COOH-	Carboxylic group
NH_2-	Amine group
CTAB	Cetyl-trimethylammonium bromide
EtOH	Ethanol
H2O	Water
$HAuCl_4 \cdot 3H_2O$	Gold (III) chloride trihydrate
HCl	Hydrogen chloride
LSPR	Localised surface plasmon resonance
MP	4-mercaptopyridine
MUA	11-mercaptoundecanoic acid
$NaBH_4$	Sodium borohydride
NaOH	Sodium hydroxide
OD	Optical density
P2VP	Poly (2-vinylpyridine)
P2VP-SH	Poly (2-vinylpyridine) with thiol terminal end group
P4VP	Poly (4-vinylpyridine)
RI	Refractive index
RIU	Refractive index unit
RPM	Revolution per minute
SAM	Self-assembled monolayer
SEM	Scanning electron microscopy
SP	Surface plasmon
SPR	Surface plasmon resonance
SPW	Surface plasmon wave

II. Acknowledgments

First of all, I feel truly grateful to have conducted 7 months of vigorous research at the Technische Universität Dresden and the Kurt-Schwabe-Institut für Mess- und Sensortechnik e.V. Meinsberg. Secondly, I would like to thank all my committee members for taking time out of their ultra-busy schedules to read my thesis and preside over my final thesis defence. Without your help this day would not be possible.

Priory I have to appreciate the chance that Prof. Dr. Patrick Wagner provided for me and connected me to such professional group in Dresden, and I would like to thank Prof. Dr. Michael Mertig for giving me the opportunity to work in his lab and intensive discussions and permanently shaping the focus of the work. I would also like to thank my supervisors for their extremely useful ideas and endless support throughout this my master thesis, Dr. Alfred Kick for his initial training with SPR device and his infinite maintenance, and Dr. Mathias Lakatos for his endless support in gold nanoparticle preparations. I would like to thank Dr. Juliane Posseckardt for her support with scanning electron microscopy (SEM) images. At last but definitely not least, I would like to thank my family and my lovely girlfriend for their support and inspiration during my study.

III. Abstract

In this thesis, a new sensor principle based on SPR is developed using AuNPs functionalised with carboxylic groups (AuNP-COOH) immobilised on self-assembled monolayers (SAM). The immobilisation of AuNP-COOHs occurs electrostatically between a positively charged SAM and negatively charged AuNP-COOHs. This SAM consists of a thiolated pH-sensitive polymer, poly (2-vinylpyridine) with a terminal thiol group (P2VP-SH), as a supporting layer on the gold surface of the SPR chip. This polymer responds to the pH changes, e.g. swelling and shrinking in acidic or basic environments, respectively. Swelling of P2VP with AuNP-COOHs occurs between pH 2.3 and 1.7. This induces an enhanced decrease of the SPR signal compared to the P2VP layers without AuNPs. This larger decrease of the SPR signal is due to the increase of the distance between the AuNPs and the gold substrate.

Additionally, other effects are measurable which allow the extension of pH sensitivity range. The further effects are related to the aggregation and disaggregation of AuNP-COOHs. At pH above 10, the SPR signal decreases strongly. It is supposed that the AuNP-COOHs disaggregate on the surface, because of the electrostatical repulsion of negatively charged carboxylic groups of the AuNPs. This assumption is verified by the immobilisation of AuNP-COOHs on 4-mercaptopyridine (MP) and cysteamine (CA) SAMs. On these monolayers, a swelling or a shrinking effect is not expected and is also not observed. However, because there are no AuNPs in the supernatant after immobilisation, signal changes on MP or CA layers are supposed to be due to the aggregation and disaggregation of AuNP-COOHs on these SAMs. A dramatic signal decrease is observed by changing the pH from neutral to a pH above 10 (disaggregation). By changing the pH from 10 to neutral and from neutral to pH below 4, the signal increases considerably (aggregation).

IV. Introduction

There are many fields of applications where pH parameter plays an important role, such as in industry, environment and biology. By the passage of time, many methods have been developed to measure the pH precisely and also to overcome the drawbacks of the prior methods [1 – 3]. For instance, pH electrode allows the simple operation in a wide range of pH values from acidic to basic with high accuracy. However, it is not appropriate for small samples due to its bulky size [4]. Even though, optical pH sensors can be miniaturized and also have adequate sensitivity, they can only be used in a limited pH range. However, many optical pH sensors which are commercially available can be used in a pH range between 5 and 9 [5]. UV-vis spectroscopy can be applied to measure the light absorption by pH-sensitive dyes at characteristic wavelengths [6]. Since an SPR sensor has been commercially introduced, numerous sensor applications have been developed in various fields of analytical chemistry, where the detection principle is not based on indicator dyes [7 – 10] but on very sensitive detection of refractive index (RI) at thin (50 nm) noble metal films (gold, silver). Therefore, most of these sensor applications are designed with surface modifications based on self-assembled monolayers containing the immobilised molecular recognition elements. These recognition elements can be chemically conjugated to gold nanoparticles (AuNP) to enhance the SPR signals [7 – 9]. In bulk solutions, AuNPs functionalised with basic or acidic functional groups aggregate and precipitate at a pH above (basic groups) or below (acidic groups) a specific value. Therefore, UV-vis can only be applied to detect a certain pH threshold value where a colloidal AuNPs dispersion is stable or not. Moreover, this precipitation is mostly irreversible.

Kick *et al.* have reported the fabrication of a polymer microarrays for pH-sensing in acidic solutions based on SPR [11]. Recently, Minko and co-workers have postulated a novel nanoscale sensor based on the swelling – shrinking effect of polymer layers, poly (2-vinylpyridine), with AuNPs [8]. They have reported that the thickness change of the polymer layers induced by pH change could significantly shift the surface plasmon absorption band due to presence of AuNPs. More recently, Sugimoto and co-workers have also investigated the swelling properties of the polymer layers with AuNPs applied in SPR biosensor applications [9]. They have reported that the molecularly imprinted polymer with immobilised AuNPs exhibited selective binding of a small molecule accompanied with swelling, which could enhance the signal.

In this thesis, the initial idea was to develop an optical label-free pH sensor which is based on pH-sensitive changes of RI in thin polymer layers. Surface plasmon resonance (SPR) sensors are optical label-free methods which are highly sensitive to RI change at the sensor surface. The RI change is due to the composition and the conformation change (swelling or shrinking) in the polymer layer. Primarily, RI change, as a consequence of conformation change, should be enhanced by gold nanoparticles (AuNP) immobilised on the pH-sensitive polymers. The distance change between AuNPs and the gold substrate is supposed to be detected with enlarged sensitivity by SPR spectroscopy. However, the interaction of the AuNPs among each other has not been considered so far. In the presented experiments, it is observed that the effect of the interaction between AuNPs dominates the signal response depending on the AuNP functionalisation.

In the present study, a new sensor principle based on SPR is developed using AuNPs functionalised with carboxylic groups (AuNP-COOH) immobilised on self-assembled monolayers (SAM). The immobilisation of AuNP-COOHs occurs electrostatically between a positively charged SAM and negatively charged AuNP-COOHs. This SAM consists of a thiolated pH-sensitive polymer, poly (2-vinylpyridine) with a terminal thiol group (P2VP-SH), as a supporting layer on the gold surface of the SPR chip. This polymer responds to the pH changes, e.g. swelling and shrinking in acidic or basic environments, respectively. It is assumed that the swelling effect of P2VP with AuNP-COOHs induces a decrease of the SPR signal, due to the increase of the distance between the AuNPs and the gold substrate. Furthermore, pH response of the AuNP-COOHs in the basic environment is studied. It is supposed that the AuNP-COOHs disaggregate on the surface, because of electrostatically repulsion of negatively charged carboxylic groups of the AuNPs. This behaviour should be verified by the immobilisation of AuNP-COOHs on 4-mercaptopyridine (MP) and cysteamine (CA) SAMs. On these monolayers, swelling or shrinking effect is not expected. However, a presumed signal change due to the aggregation and disaggregation of AuNP-COOHs on the SAMs is examined.

1. Fundamentals

1.1. Introduction to pH value and pH measurement

The term "pH" was first illustrated by the Danish biochemist Søren Peter Lauritz Sørensen in 1909 [12]. The pH stands for the “hydrogen ion exponent” where “p” stands for the mathematical symbol of the negative logarithm and “H” is the chemical symbol of hydrogen. In the era of modernity, pH value has been playing an important role in many fields, such as in medicine, biology, chemistry, agriculture, food science, nutrition and many other fields [14]. The pH describes the degree of acidity and basicity of a substance. It is measured on a scale of 0 to 14. The formal equation of pH value is described in Equation 1, which corresponds to the negative logarithm of hydrogen ion concentration [H^+] in an aqueous solution [12].

$$pH = -\log[H^+]. \quad (1)$$

The first definition of pH, where [H^+] is the hydrogen ion concentration (mol/L), was subsequently modified to

$$pH = -\log a_H, \quad (2)$$

Where a_H is the hydrogen ion activity [14].

1.1.1. pH electrode sensor

The pH meter is used in a broad field and many industrial applications [13 - 19]. Latest surveys have indicated that a conventional glass electrode apparatus can be utilised to provide accurate values of acidity in aqueous solutions, especially when only relative values of the acidity are needed [15]. The method is based on the measurement of the potential between two electrodes, a glass electrode and a reference electrode. The glass electrode, known as measuring electrode, is made of a particular glass in order to generate an ion selective barrier [16]. The reference electrode provides a constant potential at a given temperature. According to the Nernst equation, the difference between the reference potential and the potential of the pH electrode is a voltage being proportional to the pH value [14].

Although the pH electrode sensor is very robust, this system also has some major drawbacks. The temperature is one of the important factors which directly influences the cracking of the electrodes. At very high temperatures, the solution inside can begin to boil or at very low temperatures it can freeze, both will end up in the damage of the electrodes. At extreme pH values, electrodes encounter alkaline or acid errors. The alkaline errors are caused by extremely high pH value which can destroy the electrode in hours. At very high pH value, the contribution of hydrogen ions is low and therefore, the activity of sodium ions is replaced in the gel layer across the glass bulb. Consequently, the measured pH is lower than the actual pH of the solution [17]. One other unexclusive issue is the size of the electrodes. It prevents the electrodes to measure in small sample volumes. Although there has been numerous developed electrodes for this approach, still this is considered as the main problem of glass electrodes [18].

1.1.2. Optical pH sensors

In contrast to pH electrode sensors, optical sensors provide more sensitivity and selectivity in pH measurements [19]. The principle of optical pH sensors is usually based on the absorption of indicator dyes. The indicator is typically an organic dye able to change its colour over a given pH level immobilized on a layer [20]. Recently fluorescence materials are widely used to enhance the optical sensor sensitivity. The sensitivity of the sensor expressed as an optical absorption of the dyes relies upon how strongly indicator dyes can bind to an adjacent layer. In order to eliminate the leaching effect, the dyes have to be covalently bound to the matrix, but covalent bonding sometimes requires complex chemical reactions [19].

In addition, in optical fibre pH sensors, the fluorescence dyes or indicator dyes are immobilised on optical fibres. Fibre-optic pH sensors are based on induced pH changes in optical or spectroscopic properties such as absorbance, reflectance, fluorescence, energy transfer and so on. Dyes cause changes in the absorption spectrum. Therefore, the interaction between dyes and the component leads to changes in optical properties of the indicators which is detected by the fibre [21, 22].

Alike the potentiometric pH sensors, conventional optical pH sensors have their own weaknesses such as leaching and photobleaching. In addition, pH indicator dyes can have sufficient accuracy only in the limited pH range. Thus, many attempts have been made through developing pH sensors which do not use pH indicator dyes. Other pH-sensing devices, based on different pH-related properties, have also been proposed; they exploit mass changing in pH-responsive hydrogel, pH-sensitive changes of RI in polymers, pH sensors based on conducting polymers [7 - 11].

1.1.3. pH-sensitive polymers as sensor layers

The pH-sensitive polymers are those whose solubility, and conformation can be manipulated by different pH, which recently have been used in various biomedical and biochemical applications [7, 11, 23, 24]. There are two kinds of pH-responsive polymers, one with acidic groups, e.g. carboxylic groups (-COOH), which swells in a basic environment, and one with basic group, e.g. pyridine groups, which swells in acidic environment. In principle, the response happens because of their functional group which are protonated, in case of a basic functional group in pH-sensitive polymers, in the acidic environment and have the same positive ions along the chain, and therefore, the chain experiences a repulsion which leads to an extended polymer chain. This effect is called swelling [11].

Many surveys have been done to investigate the behaviour of sensitive polymers by changing the pH level. Kick *et al.* postulated that polymers with pyridine groups can be protonated and deformed in acidic environment. Polymers such as poly(2-vinylpyridine) (P2VP) and poly(4-vinylpyridine) (P4VP) are pH-sensitive polymers which express swelling effect in acidic solutions [7, 11, 25].

1.1.4. Colorimetric pH sensors

Many optical pH sensors, as mentioned in section 1.1.2, are usually made based on the analysis of fluorescence intensity, and wavelength shift, which generally requires a complicated tools. Colorimetric measurements allows with many advantages, including rapidly readable responses, and simple and doable operation approach. The colorimetric optical pH sensors are based on the colour change of the colour indicators, such as fluorescents [26]. Recently, Noble metallic nanoparticles conjugated with fluorescents have been used to indicate the colour changes due to the pH change. The pH responses are caused by the aggregation of particles and quenching of the fluorescents. UV-vis spectroscopy is used to measure the absorption peak of the fluorescent dye. The fluorescent intensity of polyethylenimine-capped with silver nanoparticles as a function of pH change is shown (Fig. 1) [27]. It is indicated that the fluorescence intensity is not measureable for very low pH values. Besides, the silver nanoclustures conjugated with fluorescents exhibit strong fluorescence intensity only in the limited range, pH 7 to 9 [27]. One of the main drawbacks of nanoparticles applied in the colorimetric pH sensors is that the solution is not reproducible. The disaggregation of the silver nanoclustures is not possible to repeat the test.

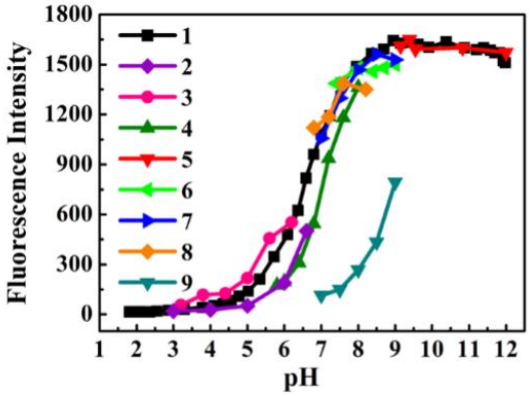

Figure 1. The pH responses of fluorescence intensities of a fluorescent-capped silver nanoclusters in different buffer solutions [27].

1.2. Surface Plasmon Resonance

1.2.1. Physics of Surface Plasmon

Surface plasmons (SP), often known as surface plasmon waves (SPW), are electromagnetic waves in the form of charge conduction oscillation that broadcast parallel across a metal/dielectric interface. SPs are transverse-magnetic (TM or p-polarised, magnetic vector is perpendicular to the plane of incidence) waves whose dispersion relation is expressed as below [28 - 30]:

$$K_{SP} = \frac{\omega}{c}\sqrt{\left(\frac{\varepsilon_d \varepsilon_m}{\varepsilon_d + \varepsilon_m}\right)}. \qquad (3)$$

Where K_{SP} is the propagation constant of the SPs, ω is the angular frequency, c is the speed of light, and ε_d and ε_m are the dielectric constant of dielectric and metal, respectively. To excite the SPs, the real part of ε_m must be negative and its magnitude must be greater than ε_d. This condition is possible in the infrared-visible wavelength region for air/metal and water/metal interfaces. Gold, silver and aluminium are some examples of those materials showing SPR effects [29]. Since ε_m is

a complex quantity, K_{SP} is indeed a complex quantity, its real part is associated with the RI and its imaginary part is related to attenuation of SPs [30]. Resonance condition, where K_x and K_{sp} are equal to exit the SP, is expressed as below:

$$K_x = \frac{2\pi}{\lambda_0} n_p \sin\theta = \mathrm{Re}\{K_{SP}\}. \quad (4)$$

Where K_x is the incident light wave vector, λ_0 is the wavelength in the vacuum, n_p is the RI of the prism, θ is the incident angle, and Re $\{K_{SP}\}$ is the real part of the propagation constant.

An evanescent electromagnetic field is connected with SP which is confined at the interface of metal/dielectric [28 - 30]. This evanescent field has a limited penetration depth into the dielectric medium. As an example, for an SP at the interface of gold layer and a dielectric with RI of 1.32, the penetration depth is typically 100-500 nm. The formula regarding the calculation of penetration depth is expressed elsewhere in literature [29].

1.2.2. Surface plasmon resonance sensor

In SPR sensors, an SP is excited by an incident light and the effect of this interaction is measured. Therefore, any change in the propagation constant of the SP, which generally is due to the RI change, can be determined. The essential factor for generating SPR by light is the conversion of photon energies into SPs [33]. This means that SPs cannot be excited directly by a light wave incident on the interface. This can be achieved by either precisely changing the angle or the wavelength of the incident light [31].The resonance angle of SPR is very sensitive to changes in the RI at the surface. These changes are used to monitor the association and dissociation of biomolecules [29].

The process is feasible by means of high RI prism coupling, corresponding to the Kretschmann SPR configuration [28]. In configurations based on prism coupling, the incident light is passed through a high RI prism and is totally reflected at the metal/dielectric interface (attenuated total reflection) causing an evanescent wave penetrating to the metal film (Fig. 2, left side) [27-29, 31]. The thickness of the metal layer must be chosen appropriately in order for evanescent wave to penetrate through metal and excite SP. Through the translation of photons to the SPs, the excitation is associated with an attenuation of reflected light intensity which can be seen as a dip in SPR spectrum (Fig. 2, right side). The angle where the intensity reaches its lowest value is called resonance angle [28 - 30]. In SPR sensors with angular modulation, an incident light with various angle of incidence is used to excite SPs. A change in RI of the sensed medium (dielectric) leads to a shift of the resonance angle (Fig. 2, right side) [29 - 31]. The relation between the resonance angle and the dielectric constant of the medium is indicated as below by the combination of equation 3 and 4:

$$n_p . \sin\theta = \sqrt{\left(\frac{\varepsilon_d \varepsilon_m}{\varepsilon_d + \varepsilon_m}\right)}. \quad (5)$$

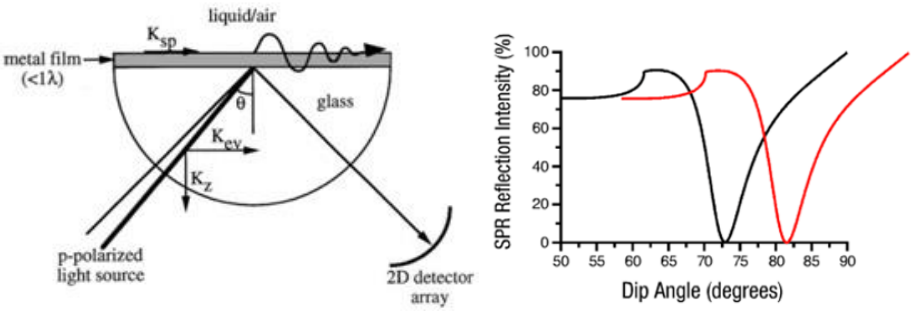

Figure 2. Kretchmann SPR system configuration and the shift in resonance angle due to RI change [32].

The RI at the surface changes by applying different type of solvent and concentration of dissolved substances, adsorption, binding, and conformation changes [9, 11, 29, and 30]. Thus, the SPR sensor is highly sensitive to small changes in RI at the surface. In this project, the SPR device from Reichert's SR7000DC SPR system has the RI resolution of 0.3 µRIU.

1.2.3. Localised Surface Plasmon Resonance

Gold nanoparticles (AuNP) with diameter larger than 3 nm can exhibit a localized surface plasmon resonance (LSPR) effect [34]. Localized surface plasmons (LSPs) are those charge density oscillations which are confined to the metallic nanoparticles (Fig. 3). LSPs can be generated directly by an electric field (light). The interaction of light with AuNP results in intense light scattering and a strong absorption band [35, 36].

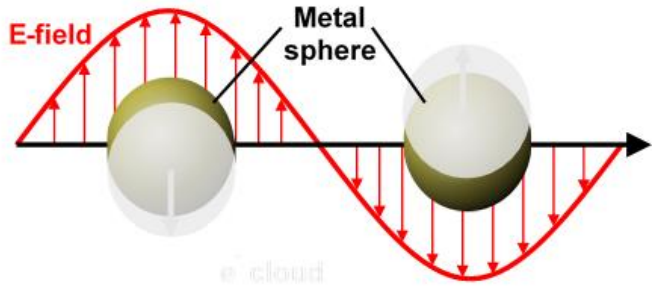

Figure 3. The SPR effect in the metal nanoparticles.

The optical properties of AuNPs can be calculated by applying Mie's theory which predicts the absorption efficiency, scattering efficiency, and optical resonance wavelengths of AuNPs [37]. These optical properties, like optical resonance wavelength, extinction cross-section, ratio of scattering and extinction coefficient, are highly dependent on AuNP size, shape and composition (material) [38]. For small AuNPs (10 nm diameter), the absorption peak is at a wavelength of approximately 520 nm and it shifts towards higher wavelength for AuNPs with bigger diameters. Also the resonant light scattering appears stronger than absorbance corresponding to the increase of the proportion of scattering coefficient in extinction coefficient for increasing particle size. The size distributions of particles leads to the broadening of SP absorption band [37 – 39].

The great interest of using AuNP in various fields has led to a huge and still increasing number of ways to prepare these gold nanoparticles. From these methods, wet chemical synthesis routes are

very promising because they are easy to manage, fast. Good results can be achieved regarding a controlled size, shape, concentration and optical properties [40, 41]. One of the common methods for AuNP preparation is the Turkevich process [43]. Herein, Au^{3+} is reduced to Au^{0} by trisodium citrate in boiling solution. The AuNPs are stabilized by a negative charged capping layer of citrate ions (Fig. 4). Further functionalization can be performed by the exchang of citrate by thiolated molecules that covalently bind to the gold surface via gold-sulphur bond. By these methods, particles can be prepared in the size range of 15 nm up to 100 nm [42]. There are a lot of other methods like seed-mediated strategies that give rise to synthesis of gold nanoparticles within a huge size range between 10 to 300 nm and different shapes [44-46].

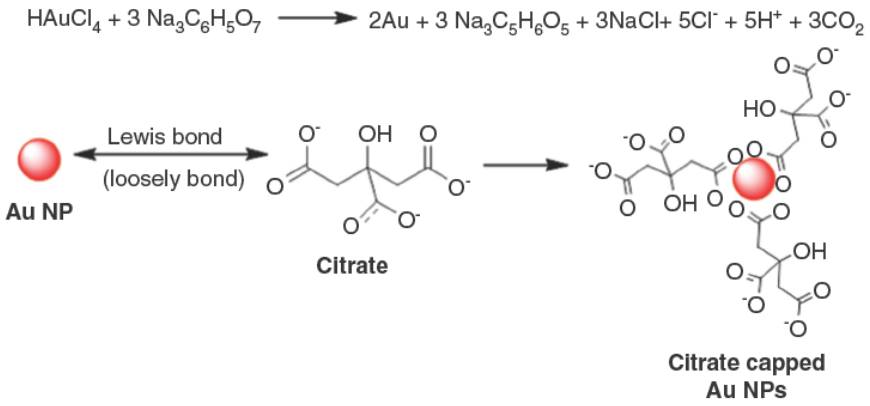

Figure 4. AuNPs formation and stabilization by Turkevich method [47].

1.2.4. Effect of AuNPs in SPR sensor

Hong *et al.* showed that LSPR of 20 nm AuNPs couple if the AuNPs are in a distance of approximately 8 nm to each other [49]. The experiments in this thesis focus on SPR investigation of AuNPs (Ø20 nm) at the proximity of a gold surface. At inter-particle distances larger than 8 nm, the adsorption of AuNPs leads only to a shift of the SPR angle. If the inter-particle is smaller than 8 nm, then the SPR angle shift is not only due to the adsorbed amounts of the AuNPs, but also the above mentioned LSPR coupling between the AuNPs has to be considered. Hong *et al.* also reported that the LSPR coupling of AuNPs to the surface plasmons at a gold film decreases with increasing distance between the AuNPs and the gold substrate [47 – 48]. This effect can significantly reduce the RI at the surface. Uchiho *et al.* calculated the resonance angle as a function of coverage with different sizes of AuNPs at two fixed wavelengths, 635, 835 nm [48]. In this work, the coverage is defined as a ratio (in %) of the area occupied by AuNPs to the corresponding total area of considered sensor surface. Uchiho *et al.* also indicated that a high coverage leads to an increase of the resonance angle (Fig. 5). Moreover, it is known that the near-fields of the AuNPs couple as a result of aggregation. Thus, considering a fixed coverage, e.g. 0.10, by aggregation of the AuNPs, the resonance angle shifts towards a larger angle. Because, it is supposed that the

effective radius of the AuNPs increases, and the LSPR coupling of AuNPs to the surface plasmons of the gold film becomes stronger (Fig. 5). As a result, the RI at the surface increases strongly.

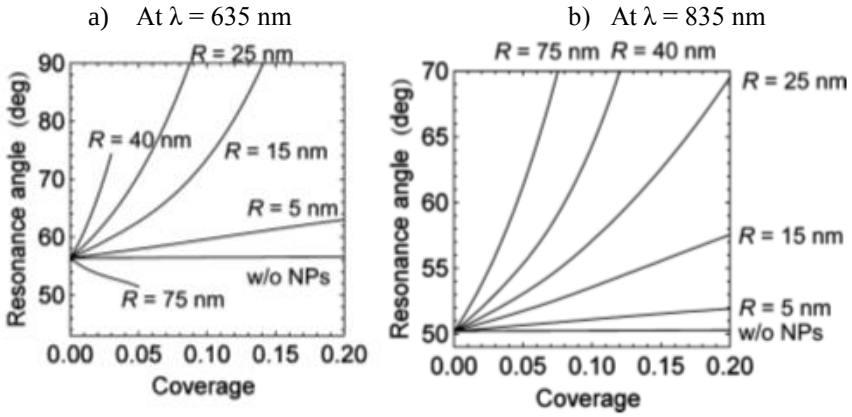

Figure 5. Calculated resonance angle as a function of coverage for different R at two fixed wavelengths, 635 and 835 nm [48].

In the present work, a Kretschmann configuration SPR setup is considered with a 50 nm thin gold layer, a self-assembled monolayer layer with thickness of d, and AuNPs with diameter of 2R functionalized with carboxylic groups (Fig. 6). The SPR measurements were performed by changing the pH of an aqueous solution at the sensor surface. Through changing the pH of the ambient medium, the polymer layer changes its conformation (swelling or shrinking).

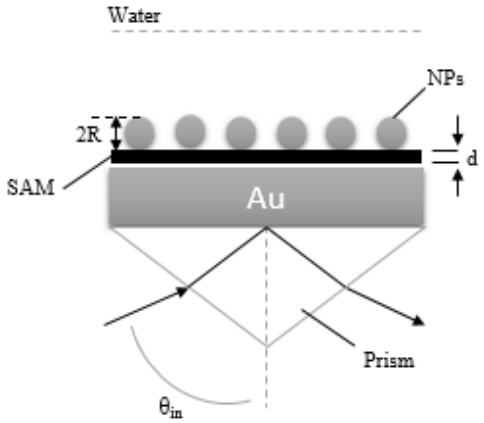

Figure 6. Schematic illustration of the sensor principle with AuNPs on SAM in SPR experiment.

The aim is to investigate the aggregation and disaggregation of the AuNPs within pH-sensitive polymer brushes at different states, e.g. swollen - shrunk. Additionally, it is assumed that the aggregation of AuNP-COOH at the swollen state of the polymer layers cannot induce changes in the SPR signal. However, the disaggregation of AuNP-COOHs at the shrunk state of the polymer layer can induce significantly large changes in the SPR signal.

2. Materials and methods

Cysteamine hydrochloride (Aldrich, 96 %), 4-Mercaptopyridine (Aldrich, 96 %), and poly (2-vinylpyridine) with thiol terminal group (P2VP-SH, Polymer source, 99%) were used for SAM formation. Hydrogen tetrachloroaurate trihydrate ($HAuCl_4.3H_2O$, Aldrich, 99.9 %), Trisodium citrate dihydrate (Sigma-Aldrich), Citric acid (Sigma-Aldrich, 99%), and Ascorbic acid (Sigma, 99%) were utilised in AuNP synthesises. 11-Mercaptoundecanoic acid (Aldrich, 97%), Sodium borohydride (NaBH4, Sigma-Aldrich, 98.5%), and Hexadecyltrimethylammonium bromide (Sigma, 99%) were used for AuNP functionalization.

UV-VIS (nanoDrop ND-2000, PEQLAB Biotechnologie GmbH) measurements were applied for investigating the absorbance of AuNPs. A multiparameter pH electrode from Mettler Toledo was used for measuring the pH value of different solutions during aggregating process.

2.1. Gold nanoparticle synthesis

Turkevich method

For the synthesis of spherical AuNP in the size range between 20 nm – 70 nm the Turkevich method was used. Therefore, 10 ml of $HAuCl_4$ (0.1 % w/v) with 90 ml deionised water was heated until it reached the boiling point. Different amounts of trisodium citrate (1 % w/v) were added to the boiling solution quickly under vigorous stirring as shown in Table. 1:

Table. 1: Summary for reaction condition of citrate reduction

Nr.	Ø NP [nm]	$HAuCl_4$ [0.1 % w/v]	dd.H_2O	Citrate [1 % w/v]	Reaction time (min)
I	10-15	10 ml	90 ml	7,0 ml	3-5
II	20-25	10 ml	90 ml	2.5 ml	3-5
III	30-35	10 ml	90 ml	1.2 ml	5-10
IV	50-60	10 ml	90 ml	1,0 ml	10-15
V	70-90	10 ml	90 ml	0.8 ml	15-25
VI	90-120	10 ml	90 ml	0.5 ml	15-25

The self-adjusting colour of the colloidal solutions varies depending on the diameter (Ø) of the nanoparticles of red (Ø = 10 nm) to orange (Ø = 100 nm). To ensure full reaction turnover and a homogeneous particle size distribution, the colloidal solutions are stirred after a successful colour change for another 30 minutes at these elevated temperatures.

2.2. Functionalization of AuNPs with carboxylic groups

For functionalization of AuNPs with carboxylic groups, 0.3 M 11-Mercaptoundecanoic acid (MUA) in 0.3 M Sodium hydroxide (NaOH) was prepared in aqueous solution. Then, 10 ml of a sample obtained from Turkevich method was used as stock solution. The stock solution was heated up to the boiling point. After that, 1 ml of citrate (1 % w/v) and 100 µl of MUA were added to the boiled solution and left overnight. After 3 to 4 days, the samples were washed. The sample

prepared with solution IV (Tab. 1) was centrifuged at 3000 RPM (revolution per minute) for 10 minutes and the sample prepared with solution II at 15000 RPM for 20 min (Tab. 1). The supernatants were replaced by deionized water. This process was repeated twice.

2.3. SPR measurements

The SPR system used in this project was from Reichert system technologies (Reichert's SR7000DC SPR system). It follows the Kretschmann configuration and contains two channels, one can be used as a reference channel and one as a measuring channel (Fig. 7). A cuvette possessing two separate chambers is placed on a 1 cm^2 gold coated SPR chip located. The chambers are sealed on the gold surface in order to prevent the solution from penetration from one to the other chamber. The capacity of the cuvette is 1.2 ml.

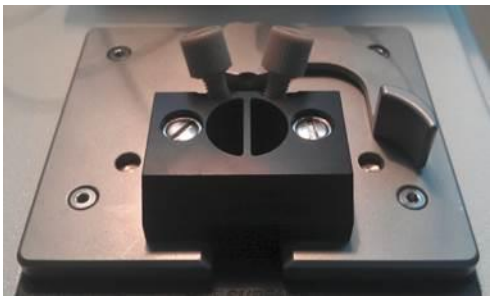

Figure 7. Reichert SPR system with cuvette SPR cell containing two chambers.

Functionalization of the SPR chip gold surfaces with cysteamine or mecaptopyridine SAMs

CA and MP were dissolved in deionised water or ethanol, respectively, to prepare a concentration of 20 mM of CA or MP. 400 µl of these solutions were placed on the gold surface of the SPR chips overnight. Afterwards, the chambers were washed with deionised water (CA) or ethanol (MP).

Experiment with cysteamine and with AuNP-COOH (Ø = 20 nm):

For immobilisation of AuNPs, two different manners were followed. 10 µl and 5 µl of the AuNPs solution with optical density (OD) of 3 (OD means the degree to which a refractive medium retards transmitted rays of light) were added in 500 µl deionized water respectively to the left and right channel. After adsorption of AuNPs, both sides were rinsed with deionised water. The HCl measurement with different concentrations (1.5, 2.85, 4.07, 23.52, and 41.16 mM) were performed on both sides. Additionally, 50 µl of AuNP stock solution was added to the right side of the surface to allow further adsorption of AuNP overnight. After rinsing with deionised water, the HCl measurement were performed with different concentrations (8, 15.68, 23.05, and 30.1 mM)

Experiment with mercaptopyridine and AuNP-COOH (Ø = 20 nm)

According to the prior experiment with CA, the adsorption of AuNPs was repeated in the same way. Thus, 10 µl and 5 µl of the AuNP stock solution (OD 3) were added in 500 µl deionised water to the left or right side of the SPR gold surface, respectively. The adsorption was stopped at the desired value of RIU by rinsing the surface with deionised water. The stability of the interaction

between AuNP-COOH and MP on the surface was checked by high concentrations of HCl and NaOH (100 mM HCl or 100 mM NaOH). After stabilisation, 50 µl of the same AuNPs stock solution was added in 450 µl deionised water to the right channel and left overnight. The aggregation and disaggregation of AuNPs were tested with NaOH and HCl measurement (Tab. 2).

Table. 2: HCl and NaOH concentrations performed on MP layer.

Composition of solution	Concentration of HCl or NaOH (mM)
H_2O	0
HCl	0.75
H_2O	0
NaOH	20.4
NaCl	20.4

Experiments with P2VP-SH with AuNP-COOH (Ø = 30 nm)

For the formation of a P2VP-SH monolayer on the SPR-sensor chip 200 µl of P2VP-SH (0.5% w/v) in EtOH was added to both chambers and was left undisturbed overnight. Next, both chambers were replaced by deionised water. The different HCl concentrations, 0.6, 1.18, 1.73, 2.79, 5.23, 7.18, 20.74, and 31.59 mM HCl, were performed. Following this, different concentrations of AuNPs were added to the two chambers of SPR cuvette. 140 µl of AuNP solution (AuNP-COOH with 30 nm diameter and OD ~ 3) was added to 250 µl deionized water into the left chamber and 20 µl of the AuNP stock solution was added to 250 µl deionized water into the right chamber. Thereby, the same HCl concentrations were implemented on the new sensor layer.

Experiments with P2VP-SH on both sides with AuNP-COOH (Ø = 20 nm) in microfluidics

A solution of 50 mM P2VP-SH was prepared in two different vials and placed into an auto sampler used for liquid handling of the SPR setup. 240 µl of these solutions were pumped in 2 h with a flow rate of 2 µl/min. The process was repeated twice. The HCl concentration test (0.1, 1, 2, 5, 10, 20, 50, 100 mM HCl) was done in microfluidics with a flow rate of 10 µl/min. 50 µl of each sample was used in 5 min. There was a 5 min gap in each step for rinsing with deionised water. For immobilisation, 20 nm AuNPs synthesised from Turkevich method functionalised with carboxylic group with OD ~ 3 were used. The process was implemented in 28 steps with 10 µl volume and 5 µl/min flow rate. The same HCl concentration was done with the same volume and flow rate (50 µl and 10 µl/min).

AuNPs desorption was tested using different concentrations of NaOH solutions. Each concentration was tested at least 3 times with volume of 5 µl and 5 µl/min flow rate. The NaOH concentrations were 0.1, 0.3, 0.5, 0.8, and 1 mM in sequence. Between each step, there was 10 min gap for rinsing with deionised water and 1 mM HCl. After performing different concentrations of NaOH, the same HCl measurement (0.1, 1, 2, 5, 10, 20, 50, and 100 mM HCl) was performed

in both channels with the same volume and flow rate (50 µl and 10 µl/min). Finally, 1 mM NaOH and 5 mM HCl concentrations were repeated 4 times to insure the reproducibility of the sensor layers.

2.4. Scanning electron microscopy

The particle sizes and shapes were derived from electron microscopy images. The scanning electron microscopy device (Helios Nanolab^{TM} 660) was from FEI Company. The voltage beam was operated at 5000 volt. For the SEM analysis, the particles were adsorbed on silicon surfaces and SPR gold chips. To study the AuNPs characterisation on a SPR gold chip, particles were adsorbed via SAMs on the SPR gold surface. The SPR gold chip was placed on a carbon substrate on a sample holder. The gold surface was connected to the sample holder via silver conductive lacquer. The characterisation of the AuNPs on SPR gold chips were more interestingly performed for analysing the coverage of the AuNPs on the surface. To study the particle sizes and shapes precisely, the AuNPs were adsorbed on silicon wafers. Briefly, a silicon wafer was cleaned by ultrasonication in ethanol and acetone for 5 min. Subsequently, a drop of concentrated AuNP solution was added onto a silicon substrate and dried in room temperature. Normally, it takes 2 h for water to evaporate completely. Finally, the sample was placed on a carbon substrate and connected to the sample holder by silver conductive lacquer. The particle sizes, shapes, and coverage were analysed by the software tool Image-j (http://imagej.nih.gov/ij).

3. Results and Discussions

3.1. AuNP characterization

In the present work, the synthesis of the AuNPs was carried out using Turkevich [43] method. In the formation of AuNPs, the colours of solutions were changed from yellow, due to reduction of Au^{3+} to Au^{0}, to ruby red colour which is the characteristic for the formation of AuNPs. It was understood that by using high amount of citrate, the AuNP sizes became smaller and more citrate was left in the solution for stabilizing the AuNPs by electrostatic repulsion due to the existence of negative charge around the shell. By using low amount of citrate, the AuNPs became bigger, but as much as the citrate concentration decreased, the mixture was less stable. As a result, it caused the higher size distribution of AuNPs (Tab. 3) expressed as standard deviation of the particle diameter analysed from SEM images. To overcome the instability of the AuNP and avoid the AuNPs aggregation in bigger sizes, after cooling down the samples, a small amount of citrate was added to each solution.

Table. 3: Average particle diameter (Ø) ± standard deviation, and wavelength (λ) of maximum absorption peak of the spherical AuNPs in sample I-III. The particle sizes were measured by image-j software.

Nr.	Volume of citrate (ml) [1 % w/v]	λ (nm)	Ø NP [nm]	# NPs analysed
I	2.5	523	23 ± 3	273
II	1.0	529	55 ± 5	81
III	0.8	535	64 ± 8	75

UV-VIS spectroscopy was used to identify and characterise the optical properties of the different AuNP sizes (Fig. 8). The relative percentage of scatter or absorption from the measured extinction spectrum depends on the size, shape, and aggregation state of particles. As a general rule, smaller particles will have higher percentage of their extinction due to absorption [38]. As can be seen in Figure 8, the absorption peak is red-shifted for bigger sizes. Also the size distribution of particles can be observed as broadening of the peak. SEM was applied to show the size, shape, and morphology of the AuNPs (Fig. 9). In the Figure 9a, the Ø20 nm AuNPs are shown with standard deviation of 3 which reveals a homogeneous size distribution. However, as can be seen in Figure 9b and 9c, size distribution of AuNPs increases (Tab. 3). Besides, the shape of the AuNPs clearly deviates from a spherical shape.

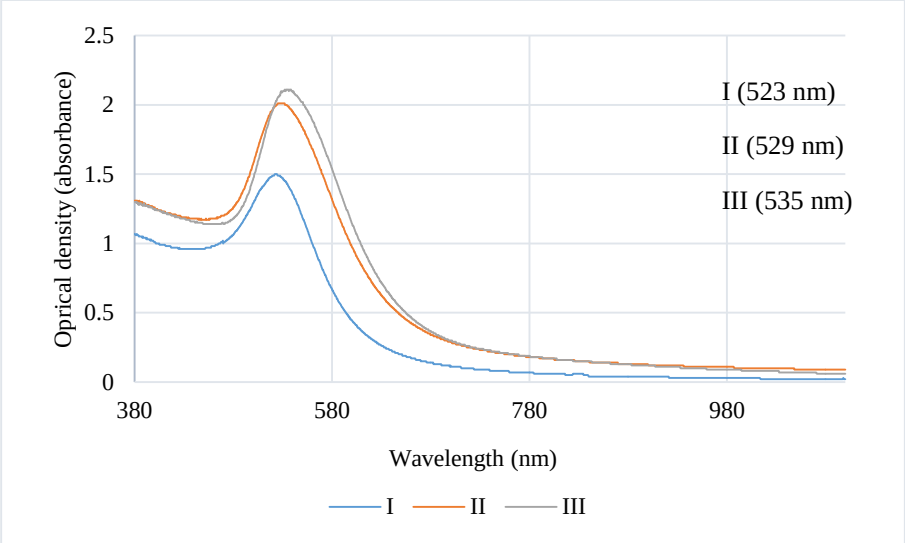

Figure 8. Extinction spectra of a set of independently prepared samples with shifted SPR peak due to a successive diameter increase. I) 2.5 ml citrate added with maximum absorption peak at 523 nm with Ø20 nm. II) 1 ml citrate added with maximum absorption peak at 529 nm with Ø55 nm. III) 0.8 ml citrate added with maximum absorption peak at 535 nm with Ø65 nm.

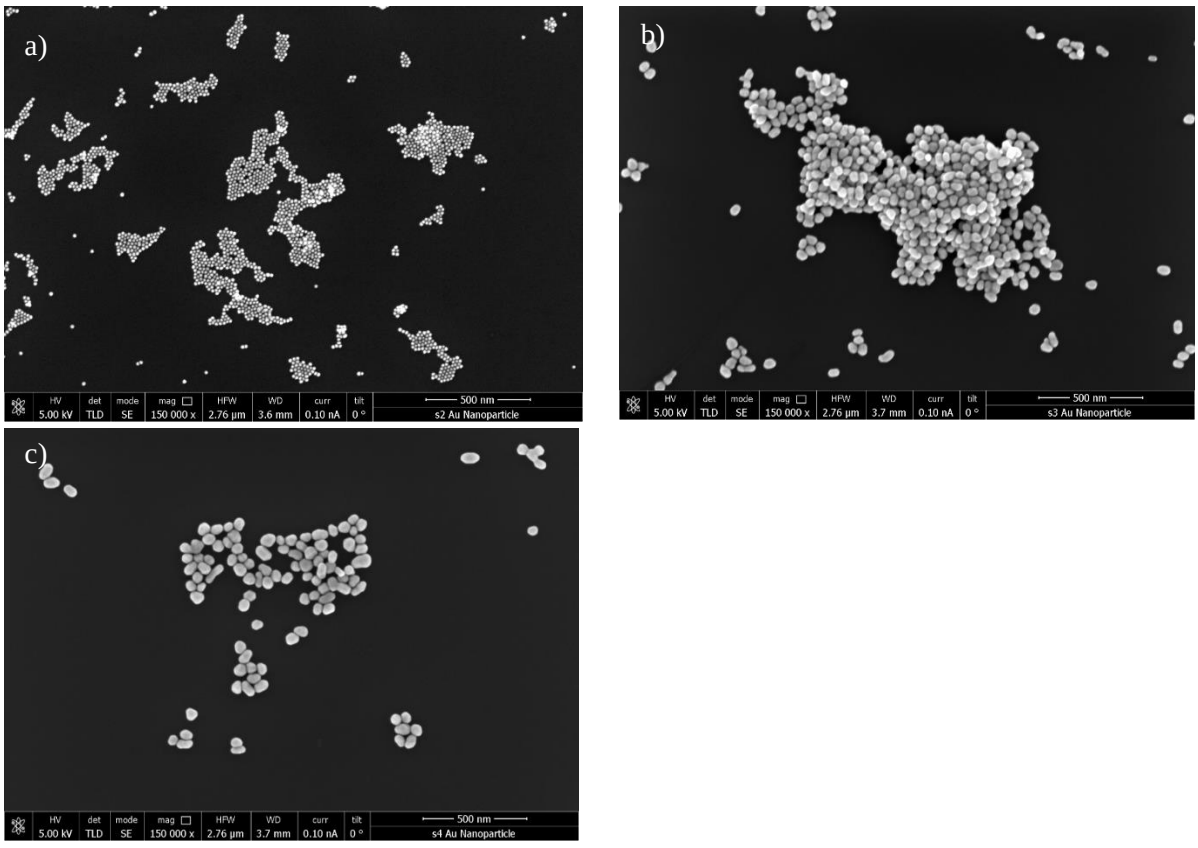

Figure 9. SEM images of AuNPs with different diameters (Ø) from samples I-III (Tab. 3) deposited on the silicon wafer. a) Ø20 nm b) Ø55 nm c) Ø65 nm

3.2. AuNP-COOH behaviour based pH in bulk solution via UV-VIS spectrsocopy

The Aggregation of AuNPs was investigated by inducing different pH values. Two samples were used for aggregation test. Two different sizes of AuNP with an OD1, Ø20 nm and Ø60 nm prepared from Turkevich method and functionalised with the carboxylic functional group were used as stock solutions. 12 vials with different pH value in the range of 0 to 14 were prepared for each AuNP sample. The pH values were measured by glass electrode pH sensor.

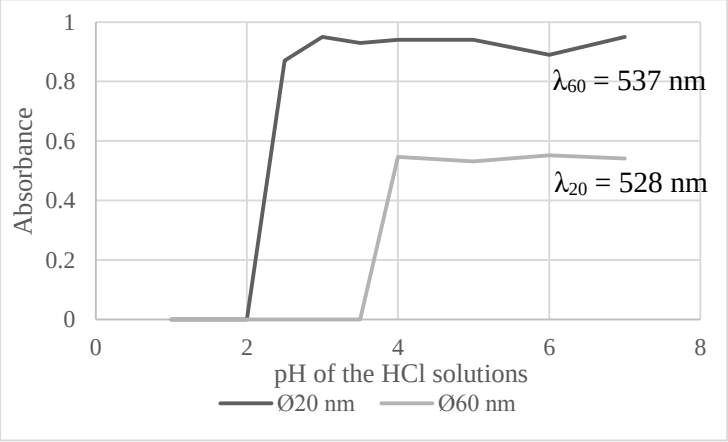

Figure 10: The pH response of absorbance at peak wavelength, λ_{20} and λ_{60}, of AuNP-COOH with Ø20 and Ø60, respectively. The absorbance is set to zero for samples where AuNPs precipitated.

It was observed that the negative charge around the shell of AuNPs from carboxyl-groups led to the high sensitivity to the acidic environment which causes the aggregation by protonation of hydrogen. The values for pH below value 2 were not measurable because of the loss in the signal (no more clear band was visible) which can be attributed to the aggregation of AuNPs (Fig. 10). In contrast, above around pH 4, no significant shift was observed. That can be explained as AuNPs with negative charge around the shell are stable in nearly basic environment. In comparison between two samples, the larger AuNPs tent to aggregate at higher pH values compared to smaller AuNPs.

It is also assumed that time can have extra influence in aggregation process. For instance, if the sample containing Ø20 nm AuNP in pH 3.5 would have left overnight, it could be possible to see the aggregation effect. Consequently, investigation of AuNPs aggregation in bulk solutions cannot precisely determine the exact pH where the AuNPs aggregate. Moreover, there was no opportunity to regenerate back the aggregated AuNPs to the same solution. Thus, the aggregation and disaggregation of AuNPs were decided to be investigated on surfaces. Because, the AuNPs have certain binding energy to the surface, and they can only move some nanometers due to the pH changes. Therefore, the aggregation and disaggregation of AuNPs can be tested at different pH values. Besides, the surface would be highly reproducible.

3.3. AuNP-COOH behaviour based pH on different surfaces

3.3.1. Ø20 nm AuNP-COOH behaviour based pH within cysteamine hydrochloride and 4-mercaptopyridine

Cysteamine (CA) and 4-mercaptopyridine (MP) were used in separate experiments as supporting layers for adsorbing AuNP-COOHs. The AuNPs with Ø20 nm were synthesised by Turkevich method. After immobilisation of the AuNPs, their adsorption strength was tested by treating the surface with NaOH solutions. First, the whole surface was covered with AuNP-COOH on a CA SAM. It was observed that the AuNPs were detached by rinsing the surface with NaOH solutions. Therefore, two surface with different coverage of AuNPs, according to their RI shift in SPR signal, were prepared (Tab. 4). The slope of the RI change measured by SPR on the mercaptoundecanol SAM (not pH-sensitive) as a function of HCl concentration quantifies the RI change in the bulk solution at the SPR sensor surface per mM HCl (Fig. 11). Therefore, it was assumed that if the surface is covered by AuNPs, an additional RI change could only be observable due to aggregation of AuNPs as a consequence of pH decrease.

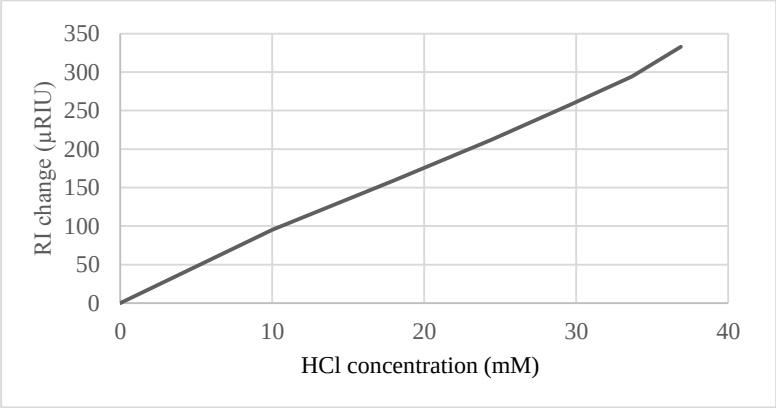

Figure 11. The measured RI change by the SPR sensor with mercaptoundecanol SAM (not pH-sensitive) as a function of HCl concentration.

Table 4: AuNP coverage and corresponding RI shift on the SPR sensor with CA SAM.

	AuNPs coverage (%)	Shift of RI (µRIU)
Left side SPR chip	1.5	1300
Right side SPR chip	5.6	2700

Following the performance of HCl test, the higher AuNP coverage resulted in bigger RI change in the acidic solutions in comparison to the lower AuNP coverage (Fig. 12). HCl solutions at the lower AuNP coverage led only to the RI change caused by the concentration dependent bulk RI of the HCl solution. Whereas, the higher AuNP coverage resulted in a larger RI change, which is assigned to the aggregation of AuNPs. Hence, this was proven as SPR signal is dependent on the

distance of AuNPs to each other, where they tend to aggregate in acidic environment and therefore they can increase the effective radius and act as a bigger particle.

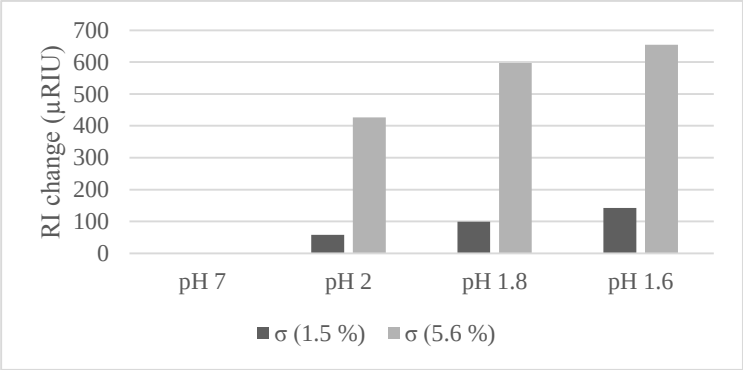

Figure 12. The RI change measured on a SPR sensor with a CA SAM as a function of pH for two different AuNP coverage (σ), 1.5 and 5.6 %.

The RI change due to the AuNPs existence on the surface for the 5.6 % coverage was approximately 2700 RIU, and the RI change with respect to 10 mM change was seen to be around 400 µRIU change. However, 10 mM HCl on a SPR sensor with mercaptoundecanol SAM (not pH-sensitive) changes the RI around 80 – 90 µRIU. This extra change of RI was assumed to be due to the aggregation of the AuNPs in the higher coverage. According the SEM images of the SPR chip, the aggregation of AuNPs could be seen clearly (Fig. 13). Figure 13a shows the surface with lower density coverage and Figure 13b indicates the surface with higher one, where the AuNPs can couple their near-fields. This aggregation occurred at pH 3.5 to 2.5. Once the AuNPs were aggregated, no further RI change in the SPR signal was seen by lowering the pH values.

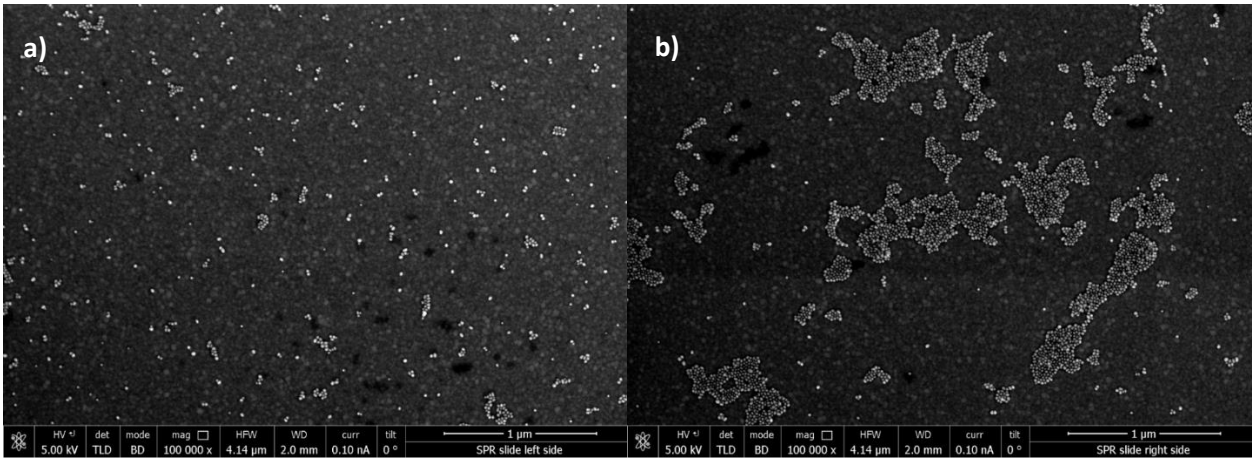

Figure 13. SEM images of Ø20 nm AuNPs self-assembled on CA SAM: a) 1.5 % coverage on the sensor surface of the left SPR channel. b) 5.6 % coverage on the sensor surface of the right SPR channel.

Next, MP SAM were used as for AuNP-COOHs immobilisation. The adsorption of AuNPs occurred greater in comparison to the CA SAM. The AuNPs were entrapped more strongly. The AuNP-COOHs on pyridine groups were not as mobile as they were on amine groups which led to the different kinetics of AuNPs adsorption. The AuNPs on the MP SAM could not be immediately

entrapped electrostatically. The strong interaction between pyridine and COO^- groups occurred over long time, overnights. Thus, a basic solution could not remove the AuNPs completely, and there were still enough particles to exhibit the extra effect of aggregation. The surface with AuNP coverage 1.6 % resulted lower RI change by changing the pH (Fig. 14a), however, the surface with AuNP coverage 6.8 % yeilded significant RI changes (Fig. 14b).

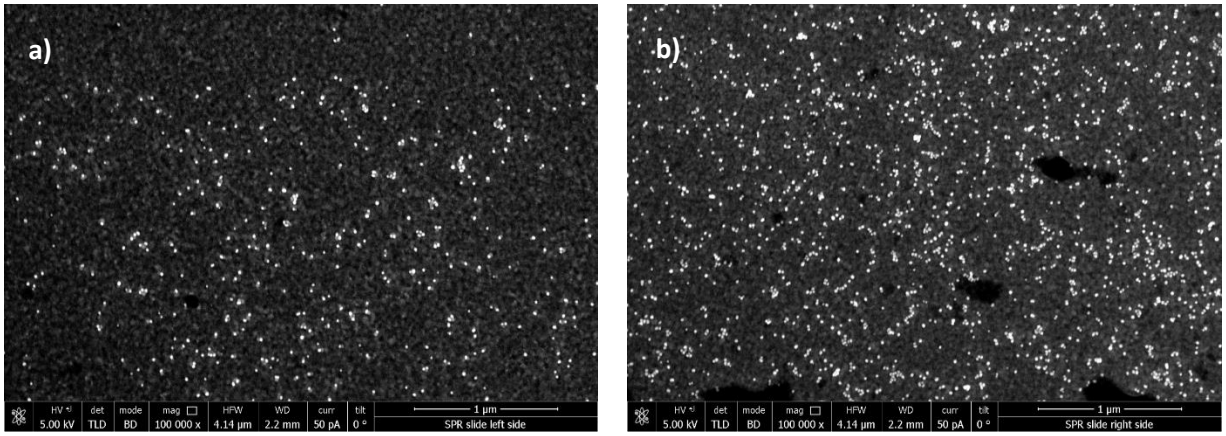

Figure 14. SEM images of Ø20 nm AuNPs self-assembled on MP: a) 1.6 % coverage on the sensor surface of the left SPR channel. b) 6.8 % coverage on the sensor surface of the right SPR channel.

In the following route, there are two absolute values for a basic (minimum) and acidic (maximum) state (Fig. 15). There are also two different RI value at the surface with water ambient medium. This was due to the background solution prior to washing with deionised water which affected the behaviour of AuNPs instead. In the acidic environment, the particles showed an attraction which caused a 1000 µRIU change in SPR signal. This could be explained by the near-field coupling of AuNPs, as there is no effect of conformation change. It was also shown that rinsing the surface after an acidic solution with deionised water could not rearrange the particles to the initial position. Thus, coming from acidic to water, the AuNPs were still close to each other within less than 8 nm in distance. However, by a basic solution, the distance between particles was enlarged, and therefore, a huge negative shift of RI in the SPR signal was observed due to the decrease of LSPR coupling of AuNPs.

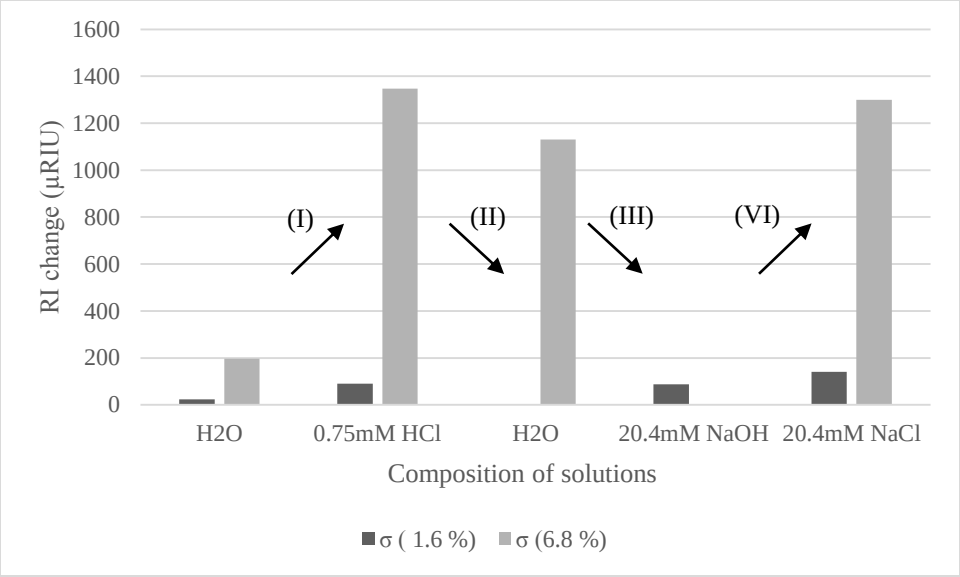

Figure 15. The RI change measured on a SPR sensor with a MP SAM as a function of pH at different AuNP coverage (σ = 6.8, and 1.6 %). I) Increasing the HCl concentration in the solution. II) Rinsing the surface with deionised water. III) Increasing the NaOH concentration in the solution. VI) Neutralising the solution by adding HCl.

The above experiments revealed that aggregation and disaggregation of AuNPs can occur at a narrow range of pH. To extend the range of pH-sensitivity, a new surface platform, based SPR, was developed using P2VP as a supporting layer for AuNP-COOH. The concept was to investigate the AuNPs effect at different states on the surface, e.g. at swollen state, or at shrunk state. In section 3.3.2, the effect of polymer self-assembling and AuNPs on the RI at the surface is shown. Later on, in section 3.3.3 and 3.3.4, the pH-sensitivity of the P2VP with and without AuNPs are tested via different HCl and NaOH concentrations.

3.3.2. SPR for Self-Assembled Monolayers (SAM) and AuNPs (Ø30 nm)

The polymer used in this master thesis was nitrogen-containing group pH-responsive polymer. This polymer shows extension in acidic solution. The self-assembly of this polymer was implemented by their thiol terminal end group. Thiols can easily bind to the gold surfaces by gold-sulphur bond. The reaction of thiols and gold surface occurs quickly within a few minutes. But, a homogeneous self-assembly of polymers occurred over long time. Therefore, the reaction must be left for a couple of hours in order to insure a maximum coverage of polymer self-assembly on the gold surface. Presence of polymers on the sensor layer causes a change in RI in the SPR signal which was seen as a shift in resonance angle (Fig. 16).

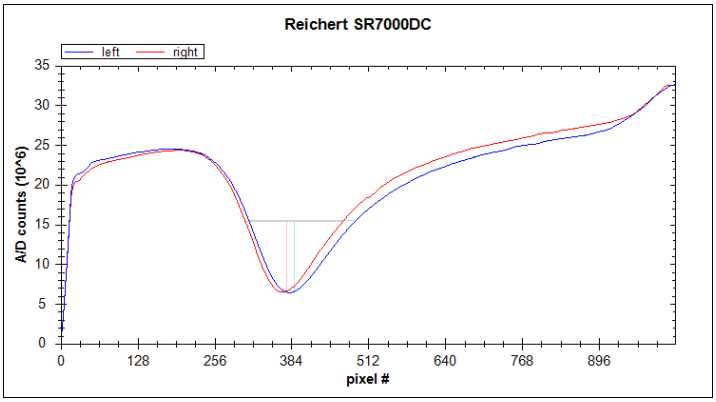

Figure 16. SPR angle spectrum on sensor surface of the right SPR channel without SAM, and on sensor surface of the left SPR channel with a P2VP-SH SAM. Reflectivity (A/D counts) shown as a function of pixel number (correlating to angle of incident).

Since polymers were assembled on a gold substrate, AuNPs-COOH (Ø30 nm) were implied to the experiment. The AuNP-COOHs were electrostatically bound to the nitrogen-containing groups of the polymers. The kinetics of AuNPs adsorption was shown differently by different concentrations of AuNPs stock solutions. As for the higher AuNP concentration, the RI in the SPR signal accelerated sharply at the beginning and after a few hours, it reached a certain slope. It must be mentioned that after almost 11 hours, the absorption of AuNPs for had not been stopped. While, the adsorption of the AuNPs in the lower concentration led to lower change in RI in the SPR signal. It also stabilized after around 2 hours (Fig. 17).

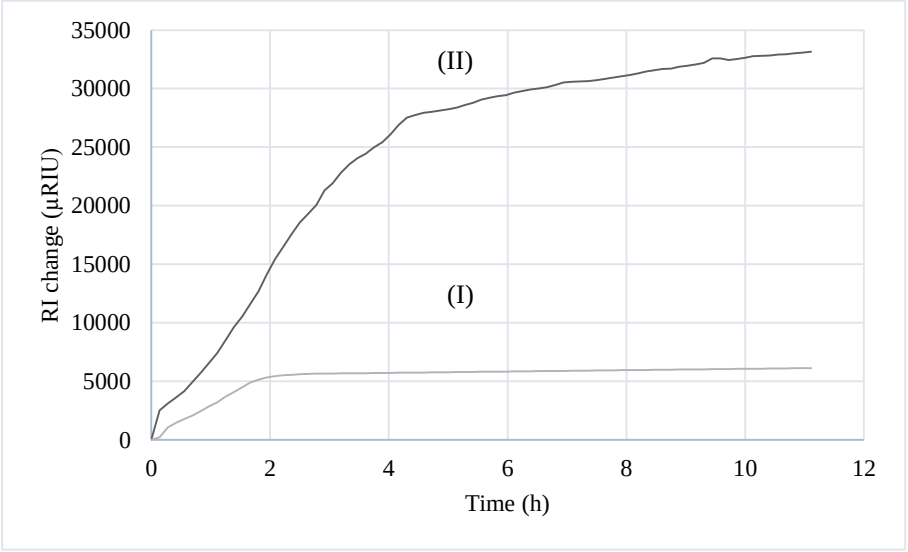

Figure 17. The kinetics of AuNPs adsorption on P2VP-SH SAM with different colloidal AuNP dispersion of two different concentrations quantified by UV-vis absorption: I) OD 0.24. II) OD 1.68.

The AuNPs adsorption on P2VP-SH SAM with different concentrations (OD 0.24, and OD 1.68) was shown by SPR measurements. The shift in the SPR angle was due to the presence of AuNPs with different coverage on the sensor SPR surface (Fig. 18). It was shown that higher coverage of

AuNPs led to the bigger shift in SPR angle. The AuNPs coverage was determined from SEM images (Fig. 19). The AuNPs coverage correlates to the shift of the SPR angle.

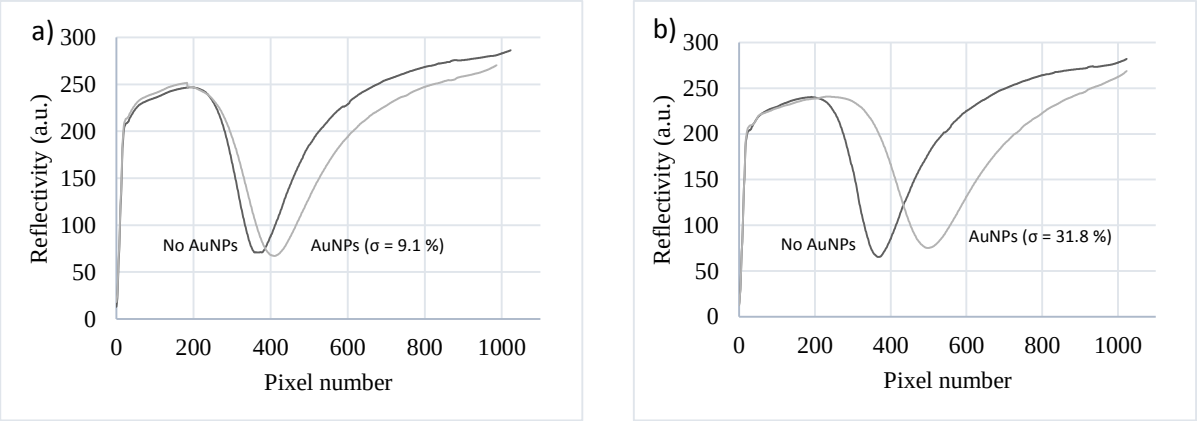

Figure 18. SPR angle spectrum with reflectivity as a function of pixel number. Pixel number correlates to the incident angle. The shift in the SPR angle due to the existence of AuNPs with Ø30 nm.

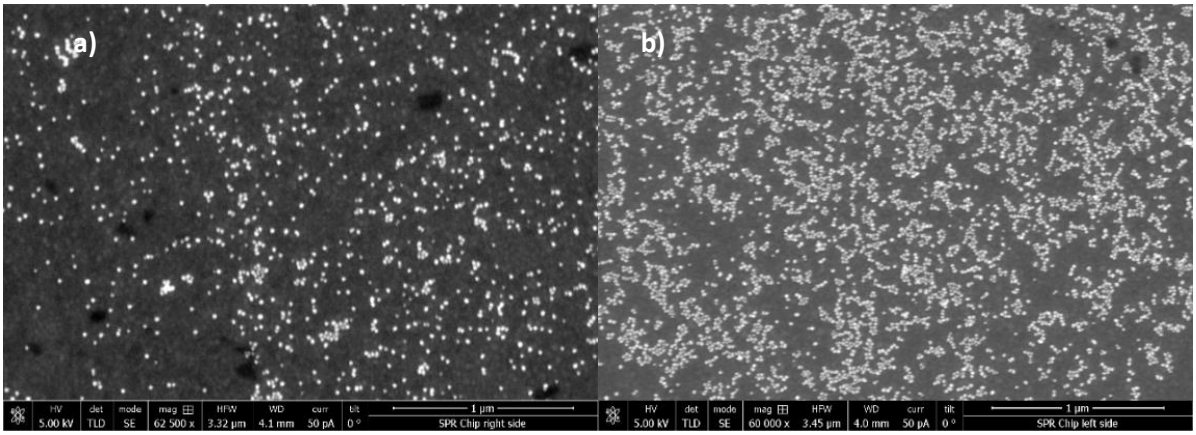

Figure 19. SEM images of Ø30 nm AuNPs self-assembled on P2VP (a) 9.1 % coverage. (b) 31.8 % coverage.

3.3.3. P2VP pH-sensitivity with Ø30 nm AuNP-COOH

Influences of the pH on the sensor with sensitive polymers had been investigated by A. Kick *et al* [11]. It could be understood that from pH between 3.5 and 2.5, the swelling effect of the P2VP appeared, however after that it could only be the uptake of HCl with different concentrations (Fig. 20) which led to the bulk RI change. Because the polymers were fully protonated and only the diffusion of ion concentration could be seen. The same sensor layer behaved differently by immobilising Ø30 nm AuNP-COOHs on pH-sensitive polymer brushes. The same concentrations of HCl solutions were used for comparing the results. The RI changes were referenced by subtracting the RI changes measured on a SPR sensor surface with a non-pH-sensitive mercaptoundecanol SAM.

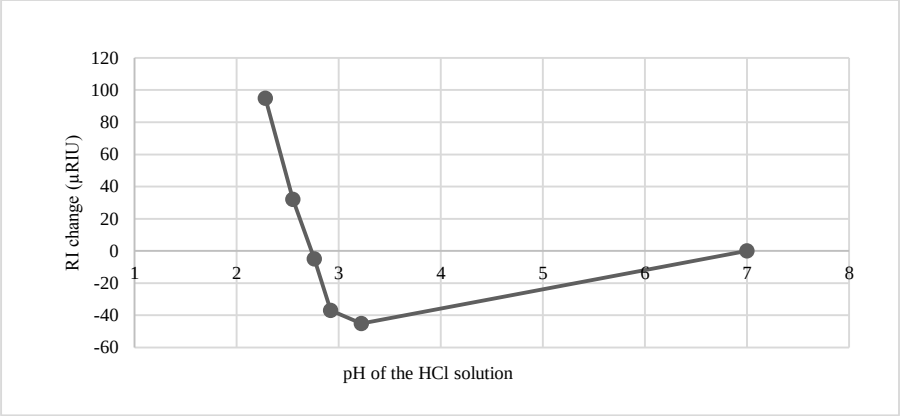

Figure 20. The RI change induced by changing the pH of the HCl solutions at the SPR sensor surface with the pH-sensitive P2VP-SH SAM. These values are referenced by subtracting the RI changes measured on a SPR sensor surface with a non-pH-sensitive mercaptoundecanol SAM.

The interaction between AuNP-COOHs and P2VP was assumed to be electrostatically due to the negative and positive charge of carboxylic and nitrogen-containing groups respectively. Therefore, by a basic solution the interaction could be disturbed. Because, the hydroxide group of a basic solution could induce negative charges along the surface and the carboxylic groups of the AuNPs could experience a repulsion. As a result, the AuNP-COOHs could detach from the P2VP. However, it was observed that a certain concentration of a basic solution, 1 mM NaOH could partially remove the AuNPs, where still around 10000 µRIU due to the AuNPs remained on the surface. The same HCl solutions tested for the surface without AuNPs were performed for the new layer with AuNPs coverage of 31.8 % (Fig. 21). It was seen that the pH-dependent SPR signal behaved completely different in comparison to the former layer. For instance, the RI in the SPR signal dramatically dropped at pH below 2.2. In that moment, this effect was not explainable. Therefore, the same sensor layer was generated in microfluidic system for more accurate measurements.

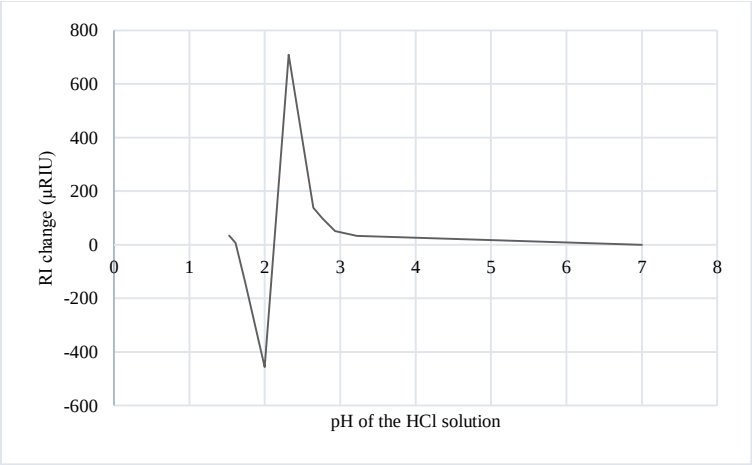

Figure 21. The RI change induced by changing the pH of the HCl solutions at the SPR sensor surface with AuNPs on P2VP-SH SAM (31.8 % coverage of AuNPs, Figure. 19).

3.3.4. P2VP pH-sensitivity with Ø20 nm AuNP-COOH in microfluidics

The same surface with P2VP was tried to be prepared in microfluidic system in order to measure more precisely and avoid contaminations on the surface. Kinetics of RI change in the SPR signal with P2VP and AuNPs in different pH values were seen more precisely. Herein, the pH-sensitivity of the P2VP without AuNPs were tested priory. It was assumed that at around pH 3, a dilution of P2VP occurred as a swelling. Thus, the swelling effect of P2VP could be seen as a decrease in the RI of the SPR signal. Following this, the adsorption of AuNPs was taken place in 28 times addition of a 10 µl of stock solution (AuNP-COOH stock solution with OD 3) with the flow rate of 5 µl/min (Fig. 22). Each step had a 10 min gap in between for rinsing with deionised water. At each step of adsorption, the RI of the SPR signal sharply increased and immediately reached the plateau. It was observed that at the three last steps, the surface was saturated by AuNPs, where no more particles could have been adsorbed. The kinetics of AuNPs adsorption could not be explained precisely. However, it was assumed that it could be due to the different concentration gradients in microfluidics, which needs further studies.

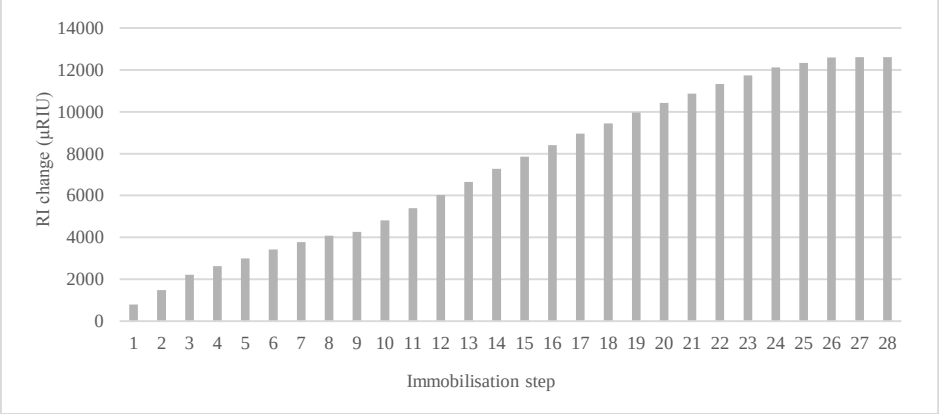

Figure 22. The RI change on P2VP-SH SAM during AuNP-COOH adsorption from a colloidal dispersion (OD 3) over 28 subsequent additions of 10 µl with flow rate of 5 µl/min.

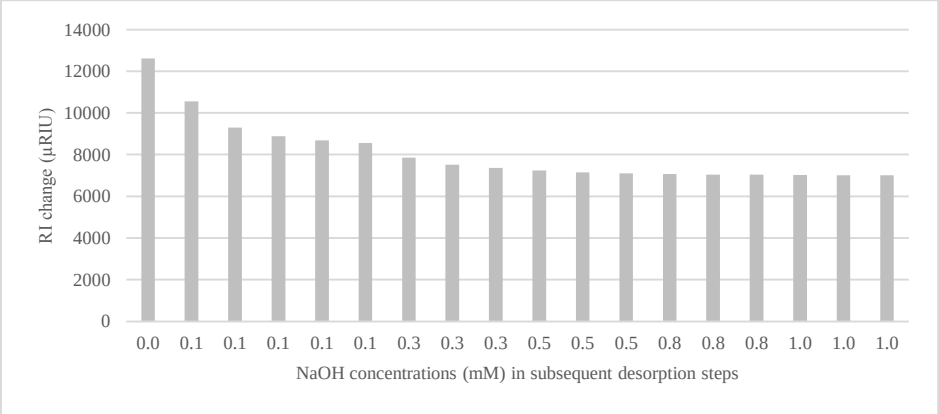

Figure 23. The RI change on P2VP-SH SAM during AuNP-COOH desorption with different NaOH concentrations 10 µl with flow rate of 5 µl/min. The RI change of the first step (0,0 mM NaOH) in water corresponds to the RI change due to amounts of immobilised AuNPs (Fig. 22, step 28).

The interaction strength between AuNPs and P2VP was tested using different concentrations of NaOH solutions (Fig. 23). Each concentration of NaOH solutions was repeated three times and had a 10 min gap for rinsing with deionised water. In the three first steps of NaOH solutions (0.1 mM), the largest detachment of the AuNPs occurred (Fig. 23). However, after that, only a slight desorption of AuNPs was observed, where it reached the stability after addition of 0.3 mM NaOH solutions. It was understood that the remained AuNPs on the surface could not be detached even with 1 mM NaOH solutions. Finally, a AuNP coverage of 3.2 % remained on the surface, which could indeed result in a enhanced SPR signal (Fig. 24).

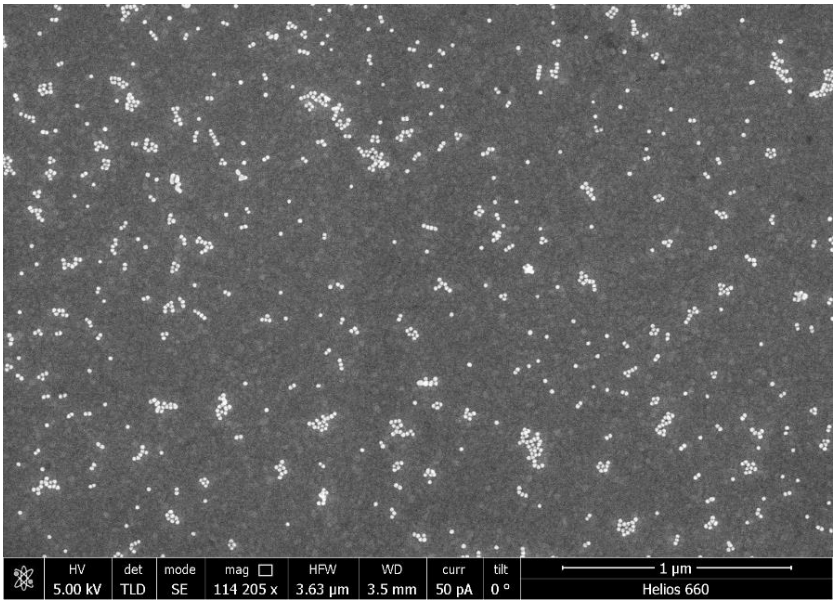

Figure 24. SEM images of Ø20 nm AuNPs self-assembled on P2VP-SH SAM with 3.2 % coverage.

The surface covered by remaining AuNPs was tested with different pH solutions for investigation of sensitivity of the surface. The pH-sensitivity of the layer containing P2VP with and without AuNPs was compared (Fig. 25). It was observed that the RI change of the SPR signal on the SPR sensor surface with AuNP (3.2 % coverage) due to the pH change was different in comparison to the layer without AuNPs. For the SPR sensor surface with only P2VP SAM, the swelling effect was assumed to occur at pH 3. It was seen that the swelling of P2VP SAM with AuNP-COOHs occurs between pH 2.3 and 1.7. The shifting of the swelling state to the lower pH was supposed to be due to the protonation of carboxylic groups on the AuNPs on the surface. Moreover, the swelling effect of the P2VP with AuNPs resulted in an enhanced decrease of the SPR signal compared to the SPR sensor surface without AuNPs. This larger decrease of the SPR signal was due to the increase of the distance between the AuNPs and the gold substrate. Because, there were weaker LSPR coupling to surface plasmons of the gold film. Furthermore, the RI at pH below 1.3 increased with the same slope as on the surface with P2VP without AuNPs.

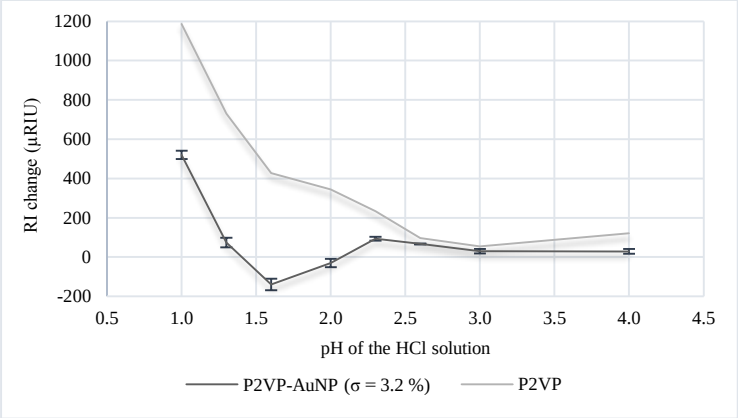

Figure 25. The RI change induced by changing the pH of the HCl solutions at the SPR sensor surface with (σ = 3.2 %) and without AuNPs on P2VP-SH SAM. Standard deviation from three measurements.

For evaluating the strength of the remained AuNPs on the layer, a certain concentration of NaOH and HCL was used. The behaviour of the layer was completely reproducible by changing the pH into basic and acidic environment (Fig. 26). The layer was highly sensitive toward a high pH value (pH 11). By an addition of 5 µl of 1 mM NaOH, the RI in the SPR signal dropped approximately 900 µRIU and it climbed up simply by a deionised water rinsing. Also, 5 mM HCl was considered as a concentration, where neither the swelling effect could occur nor the aggregation of AuNPs. Therefore, the accelerated signal was assumed to be only the protonation of the layer and bulk RI change.

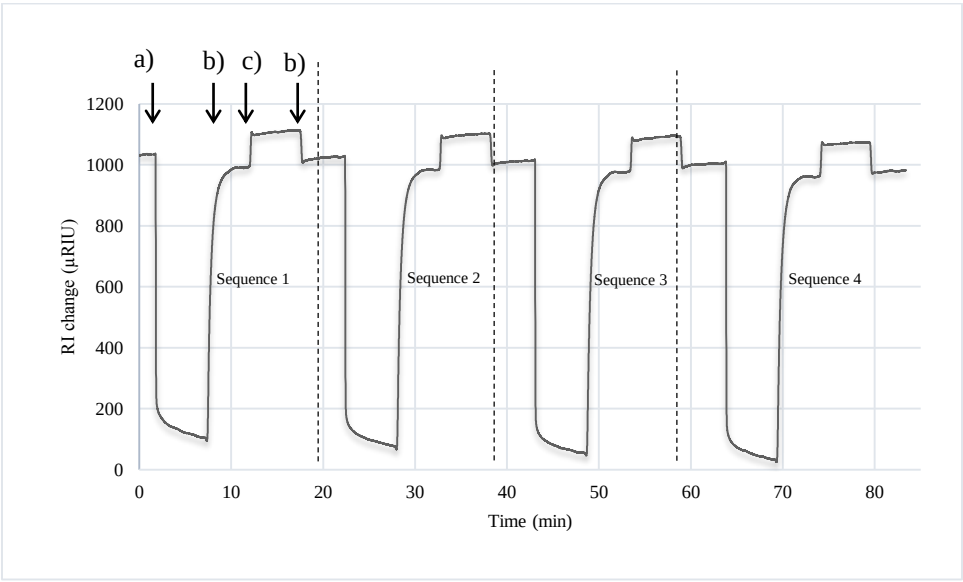

Figure 26. Kinetics of RI change on P2VP-SH SAM with AuNP (3.2 % coverage). Water, HCl, and NaOH solutions were pumped over the SPR sensor surface in the order: a) 1 mM NaOH, b) water, c) 5 mM HCl, d) water. This sequence was repeated 4 times.

Thereby, the swelling and shrinking of the polymer and aggregation and disaggregation of the AuNPs can be observed from this schematic illustration (Fig. 27). These two effects behave

oppositely, where the AuNPs aggregate while the polymer layers swell and vice versa. The behaviour of the AuNP-COOHs in a basic solution can be expressed as disaggregation effect which dominates the shrinkage effect of the polymer layers. In the basic environment, the negative charges between the AuNP-COO^- increases and leads to a repulsion between particles. As known from the literature [49], 20 nm AuNPs cannot couple their LSPR in distance greater than 8 nm. Thus, in a basic environment the repulsion of the AuNPs takes place in only some nanometers. As a consequence, the RI at the surface drops sharply. The response of the developed sensor is highly reproducible.

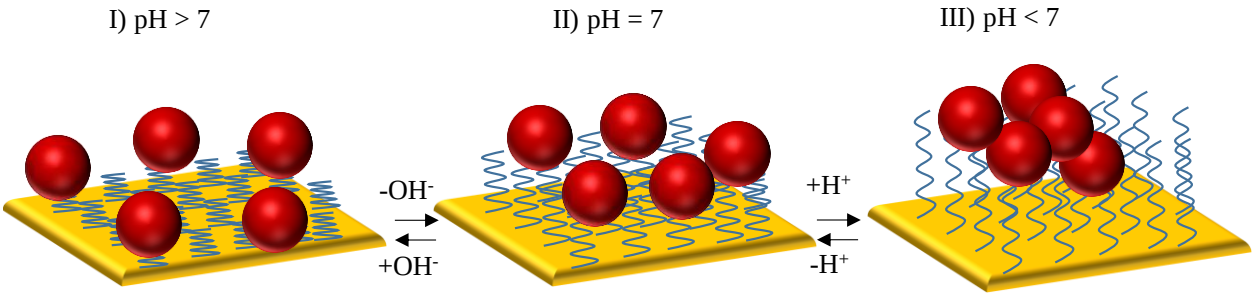

Figure 27. The schematic illustration of working principle of the developed sensor surface with AuNP-COOHs immobilised on P2VP-SH SAM. I) Electrostatic repulsion and disaggregation of AuNPs accompanied by shrinkage of the P2VP chains at pH > 7. II) At pH = 7, the P2VP chains are partly swollen and the AuNPs can approach each other. III) Aggregation of the AuNPs accompanied by the complete swelling of P2VP chains at pH < 7.

In basic environment, AuNPs are in maximum distance to each other, more than 8 nm, where the near-field coupling cannot occur. As a result, the RI at the SPR sensor surface decreases. In acidic environment, the AuNPs aggregate. However, their distance to the gold substrate is enhanced due to swelling of the polymer chains. Consequently, the LSPR coupling of the AuNPs to the SPR of the gold surface decreases, and therefore, the RI at the SPR sensor surface decreases [48, 49].

4. Conclusions and outlook

The aggregation and disaggregation of AuNPs were investigated in bulk solutions and on surfaces. UV-VIS spectroscopy was applied to characterise the aggregation of AuNPs in bulk solutions. The precipitation occurred irreversibly during the aggregation of AuNP-COOH in bulk. SPR spectroscopy was used for monitoring the effect of AuNPs on the sensor layers. The behaviour of AuNPs with respect to the pH changes was shown on different SAM surfaces. It was seen that pyridine groups, either in P2VP or MP, were considered as proper layers for AuNPs adsorption. Also, CA were tested as a holding layer for AuNPs, while the interaction between carboxylic group of AuNPs and amine groups of CA was found to be much weaker. The AuNPs could be removed from the holding layer almost completely via a basic solution. As known, the MP have no opportunity to swell and by changing the pH, only the protonation and deprotonation of the pyridine group could happen. Thus, the AuNP-COOHs on the MP can only aggregate and disaggregate on the surface which could be seen as a sharp positive and negative RI shift in the SPR signal, respectively. P2VP layers, on the other hand, had additional effect of swelling and shrinking effect due to the pH changes. The AuNP-COOHs on the P2VP could aggregate in acidic environment, while the polymer layers at certain pH swelled. The swelling of the polymer led to the increase of the distance between AuNPs and gold substrate which was assumed to be the reason of RI drop in the signal. AuNPs at longer distance to gold substrate have weaker LSPR coupling the surface plasmons of the gold substrate. Therefore, at pH between 2.3 and 1.7, the SPR signal strongly negatively enhanced. In the basic environment, the RI in the signal also decreased dramatically. Although, at high pH alues the polymer shrank and AuNPs became close to the surface, the AuNPs could experience disaggregation. Hence, by disaggregation of AuNPs, the RI at the surface decreased sharply. To quantify which decrease of the RI at the surface would belong to AuNP disaggregation or polymer layer swelling, the behaviour of a pH-sensitive polymer brushes without AuNPs in the same situation could be considered simultaneously as a reference value.

In the ongoing studies, the range of pH-sensitivity can be varied by applying different pH-responsive polymers, which have acidic groups (-COOH) and AuNPs functionalised with different functionalities, e.g. $–NH_2$. Therefore, a new sensor could be developed with different pH-sensitivity ranges. Based on the current achievement, the adsorption of AuNPs were dependent on the density of the polymer film. It was assumed that the charge density over the polymer layer plays important role for entrapping the AuNP-COOHs electrostatically. Thus, the charge density of the layer needs further studies for precisely determine the AuNPs adsorption. Moreover, AuNPs with bigger sizes are assumed to change the SPR signal greater than smaller AuNPs due to larger LSPR coupling to the surface plasmons of the gold surface. Besides, AuNPs with octahedral, rod, and triangle, or other shapes can shift the plasmon wavelength differently. Thus, applying AuNPs with different shapes and sizes on the surfaces can be compared to the current achievements with the spherical AuNPs.

Reference

1. O. K. Khalil A. Edric G and Arousian A. Review on State-of-the-art in Polymer Based pH Sensors. Sensors 2007, 7, 3027-3042.
2. J. Janata Do optical sensors really measure pH. Analytical Chemistry, 1987, 59, 1351-1356.
3. K. Arshak, E. Gill, A. Arshak, and O. Korostynsk. Investigation of tin oxides as sensing layers in conductimetric interdigitated pH sensors. Sensors and Actuators B: Chemical 2007, 127, 42-53.
4. E. Bakker and A. Xu, E. Pretsch. Optimum composition of neutral carrier based pH electrodes. Analytica Chimica Acta, 1994, 295, 253-262.
5. D. Wencel, B.D. MacCraith, and C. McDonagh. High performance optical ratiometric sol–gel-based pH sensor. Sensors and Actuators, 2009, 139, 208-213.
6. I. Grabchev, I. Moneva, V. Bojinovb and S. Guittonneauc. Synthesis and properties of fluorescent 1,8-naphthalimide dyes for application in liquid crystal displays. J. Mater. Chem., 2000,10, 1291-1296.
7. A. Kick and M. Mertig. Characterization of pH-sensitive polymer layers by surface plasmon resonance and quartz crystal microbalance. Phys. Status Solidi A, (2015), DOI 10.1002/pssa.201431604.
8. I. Tokareva, S. Minko, J. H. Fendler, and E. Hutter. Nanosensors Based on Responsive Polymer Brushes and Gold Nanoparticle Enhanced Transmission Surface Plasmon Resonance Spectroscopy. J. AM. CHEM. SOC. 2004,126, 15950-15951.
9. J. Matsui, K. Akamatsu, N. Hara,D. Miyoshi,H. Nawafune, K. Tamaki, and N. Sugimoto. SPR Sensor Chip for Detection of Small Molecules Using Molecularly Imprinted Polymer with Embedded Gold Nanoparticles. Anal. Chem. 2005, 77, 4282-4285.
10. K. Kuriara and K. Suzuki. Theoretical Understanding of an Absorption-Based Surface Plasmon Resonance Sensor Based on Kretchmann's Theory. Analytical chemistry. 2002, 74, 696-701.
11. A. Kick and M. Mertig. Polymer Microarrays for Surface Plasmon Resonance Based Sensors. Sensors IEEE. 2014, 2086 – 2088.
12. S.P.L. Sørensen, Études enzymatiques. II. Sur la mesure et l'importance de la concentration des ions hydrogène dans les réactions enzymatiques, Biochemische Zeitschrift, 1909, 21, 131-304.
13. W. Gaoa, W. W. Tjiub, J. Weia, and T. Liu. Highly sensitive nonenzymatic glucose and H2O2 sensor based on Ni(OH)2/electroreduced graphene oxideMultiwalled carbon nanotube film modified glass carbon electrode. Talanta, 2014, 120, 484-490.
14. A.K. Covington, R. G. Bates, and R. A. Durst. Definition of pH scales, standard reference values, measurement of pH and related terminology. Pure & Appl. Chem. 1985, 57, 531-542.
15. H. Nilsson, A-CAkerlund, and K. Mosbach. Determination of glucose, urea and penicillin using enzyme-pH-electrodes. BBA General Subjects, 1973, 320, 529-534.
16. K. G. Kreider, M. J. Tarlov, and J. P. Cline. Sputtered thin-film pH electrodes of platinum, palladium, ruthenium, and iridium oxides. Sensors and Actuators B: Chemical, 1995, 28, 167-172.
17. P. K. Glasoe and F. A. Long. Use of glass electrodes to measure acidities in deuterium oxide. J. Phys. Chem, 1960, 64, 188-190.
18. M. Dole. The early history of the development of the glass electrode for pH measurements. *J. Chem. Educ.*, 1980, 57, 134.
19. F. Luca, R. Luigi, F. Paola and P. Francesco. Disposable Fluorescence Optical pH Sensor for Near Neutral Solutions. Sensors 2013, 13, 484-499.
20. Z. Jin, Y. Su, and Y. Duan. An improved optical pH sensor based on polyaniline. Sensors and Actuators B, 2000, 71, 118-122.
21. B. Gu, Y. Ming-Jie, A. Ping Zh, Jin-Wen Q and Sailing He. Low-cost high-performance fiber-optic pH sensor based on thin-core fiber modal interferometer. Fiber optics sensors, 2009, 17, 22296-222302.
22. S. K. Mishra and B. D. Gupta. Surface plasmon resonance based fiber optic pH sensor utilizing Ag/ITO/Al/hydrogel layers. Analyst, 2013,138, 2640-2646.

23. S. H. Hong, S. W. Hong, and W. H. Jo. A new polymeric pH sensor based on photophysical property of gold nanoparticles and pH sensitivity of Poly(sulfadimethoxinemethacrylate). Macromol. Chem. Phys. 2010, 211, 1054–1060.
24. S. Dai, P. Ravi, and K. Ch. Tam. pH-responsive polymers: Synthesis, properties and applications. Soft Matter, 2008, 4, 435–449.
25. S. P. Adiga, and D. W. Brenner. Stimuli-Responsive Polymer Brushes for Flow Control through Nanopores. *J. Funct. Biomater.* 2012, *3*, 239-256.
26. H. Chena, X. Wanga, X. Songa, T. Zhoua, Y. Jianga, and X Chen. Colorimetric optical pH sensor production using a dual-colour system. Sensors and actuators. 2010, 146, 278-282
27. F. Qu, N. Bing Li, and H. Q. Luo. Highly Sensitive Fluorescent and Colorimetric pH Sensor Based on Polyethylenimine-Capped Silver Nanoclusters. Langmuir. 2013, 29, 1199-1205.
28. Kretschmann E; Raether, H. Zeitschrift Fur Naturforschung Part aAstrophysik Physik Und Physikalische Chemie 1968, A 23, 2135-2136.
29. J. Homola, S. Sinclair, and Y. Günter Gauglitz. Surface plasmon resonance sensors: review. Sensors and Actuators B: Chemical. 1999, 54, 3-15.
30. P. Lecaruyer, E. Maillart, M. Canva, and J. Rolland. Generalization of the Rouard method to an absorbing thin-film stack and application to surface plasmon resonance. Applied Optics, 2006, 45, 8419-8426.
31. A.V. Nabok, A. Tsargorodskaya, A.K. Hassan, and N.F. Starodub. Total internal reflection ellipsometry and SPR detection of low molecular weight environmental toxins. Applied surface science, 2005, 246, 381-386.
32. (http://jlocklin.uga.edu/research.html) 16.04.2015.
33. R.D. Harris, and J.S. Wilkinson. Waveguide surface plasmon resonance sensors. Sensors and actuators. 1995, 29, 261-267.
34. CS. onnichsen, T. Franzl, T. Wilk, G von Plessen and J Feldmann. Plasmon resonances in large noble-metal clusters. New Journal of Physics 4 (2002) 93.1–93.
35. K. Lance Kelly, Eduardo Coronado, Lin Lin Zhao, and George C. Schatz. The Optical Properties of Metal Nanoparticles: The Influence of Size, Shape, and Dielectric Environment. J. Phys. Chem. B 2003, 107, 668-677.
36. K. Minami, H. Sakaue, Sh. Shingubara and T. Takahagi. Optical spectroscopic studies of the dispersibility of gold nanoparticle solutions. J.Appl.Phys, 2002, 92, 7486-7490.
37. P. K. Jain, K. S. Lee, Ivan H. El-Sayed, and Mostafa A. El-Sayed. Calculated Absorption and Scattering Properties of Gold Nanoparticles of Different Size, Shape, and Composition: Applications in Biological Imaging and Biomedicine. J. Phys. Chem. B 2006, 110, 7238-7248.
38. I. H. El-Sayed, X. Huang and M. A. El-Sayed. Surface Plasmon Resonance Scattering and Absorption of anti-EGFR Antibody Conjugated Gold Nanoparticles in Cancer Diagnostics: Applications in Oral Cancer. Nano Lett., 2005, 5,829–834.
39. P. N. Njoki, I-Im S. Lim, D. Mott ,Hye-Y.Park, B. Khan, S. Mishra ,R. Sujakumar, Jin Luo, and C-J. Zhong. Size Correlation of Optical and Spectroscopic Properties for Gold Nanoparticles. J. Phys. Chem. *C*, 2007, 111, 14664–14669.
40. J. Zhou, J. Ralston, R. Sedev and D. A. Beattie. Functionalized gold nanoparticles: Synthesis, structure and colloidal stability. Journal of Colloid and Interface Science 331, 2009, 251–262.
41. H. N. Verma , P. Singh and R. M. Chavan. Gold Nanoparticles: Synthesis and characterization. Veterinary world, 7(2), 72-77.
42. J. Kimling, M. Maier, B. Okenve, V. Kotaidis, H. Ballot, and A. Plec. Turkevich Method for Gold Nanoparticle Synthesis Revisited. J. Phys. Chem. B 2006, 110, 15700-15707.
43. J. Turkevitch, P. C. Stevenson and J. Hillier. A study of the nucleation and growth processes in the synthesis of colloidal gold. Discuss. Faraday Soc., 11, 55 (1951). 9, 33, 131.
44. Ch. Ziegler and A. EychmuellerSeeded growth synthesis of uniform of gold nanoparticles with diameter of 15-300 nm. J. Phys. Chem. C 2011, 115, 4502-4506.

45. N. G. Bastus, J. Comenge and V. Puntes. Kinetically Controlled Seeded Growth Synthesis of Citrate-Stabilized Gold Nanoparticles of up to 200 nm: Size Focusing versus Ostwald Ripening. Langmuir, 2011, 27, 11098-11105.
46. N. R. Jana, L. Gearheart and C. J. Murphy. Seeding growth for size control of 5-40 nm diameter gold nanoparticles. Langmuir, 2001, 17, 6782-6786.
47. S. Szunerits, J. Spadavecchia and R. Boukherroub. Surface plasmon resonance: signal amplification using colloidal gold nanoparticles for enhanced sensitivity. Rev Anal Chem 2014, 33, 153–164.
48. Y. Uchiho, M. Shimojo, K. Furuya, and K. Kajikawa. Optical Response of Gold-Nanoparticle-Amplified Surface Plasmon Resonance Spectroscopy. J. Phys. Chem. C 2010, 114, 4816–4824.
49. X. Hong, and E. A. H. Hall. Contribution of gold nanoparticles to the signal amplification in surface plasmon resonance. Analyst, 2012, 137, 4712-4719.

Auteursrechtelijke overeenkomst

Ik/wij verlenen het wereldwijde auteursrecht voor de ingediende eindverhandeling:
Surface plasmon resonance investigation of gold nanoparticle aggregation on self-assembled monolayers

Richting: **master in de biomedische wetenschappen-bio-elektronica en nanotechnologie**
Jaar: **2015**

in alle mogelijke mediaformaten, - bestaande en in de toekomst te ontwikkelen - , aan de Universiteit Hasselt.

Niet tegenstaand deze toekenning van het auteursrecht aan de Universiteit Hasselt behoud ik als auteur het recht om de eindverhandeling, - in zijn geheel of gedeeltelijk -, vrij te reproduceren, (her)publiceren of distribueren zonder de toelating te moeten verkrijgen van de Universiteit Hasselt.

Ik bevestig dat de eindverhandeling mijn origineel werk is, en dat ik het recht heb om de rechten te verlenen die in deze overeenkomst worden beschreven. Ik verklaar tevens dat de eindverhandeling, naar mijn weten, het auteursrecht van anderen niet overtreedt.

Ik verklaar tevens dat ik voor het materiaal in de eindverhandeling dat beschermd wordt door het auteursrecht, de nodige toelatingen heb verkregen zodat ik deze ook aan de Universiteit Hasselt kan overdragen en dat dit duidelijk in de tekst en inhoud van de eindverhandeling werd genotificeerd.

Universiteit Hasselt zal mij als auteur(s) van de eindverhandeling identificeren en zal geen wijzigingen aanbrengen aan de eindverhandeling, uitgezonderd deze toegelaten door deze overeenkomst.

Voor akkoord,

Khangholi, Navid

Datum: **9/06/2015**